

**This is the accepted manuscript version of the contribution published as:**

Schwöbel, J.A.H., Ebert, A., Bittermann, K., Huniar, U., Goss, K.-U., Klamt, A. (2020):  
COSMOperm: Mechanistic prediction of passive membrane permeability for neutral  
compounds and ions and its pH dependence  
*J. Phys. Chem. B* **124** (16), 3343 – 3354

**The publisher's version is available at:**

<http://dx.doi.org/10.1016/j.agee.2020.106927>

## B: Biomaterials and Membranes

**COSMO<sub>perm</sub>: Mechanistic Prediction of Passive Membrane Permeability for Neutral Compounds and Ions, and its pH Dependence**

Johannes Schwöbel, Andrea Ebert, Kai Bittermann, Uwe Huniar, Kai-Uwe Goss, and Andreas Klamt

*J. Phys. Chem. B*, **Just Accepted Manuscript** • DOI: 10.1021/acs.jpcc.9b11728 • Publication Date (Web): 27 Mar 2020Downloaded from [pubs.acs.org](https://pubs.acs.org) on April 7, 2020**Just Accepted**

“Just Accepted” manuscripts have been peer-reviewed and accepted for publication. They are posted online prior to technical editing, formatting for publication and author proofing. The American Chemical Society provides “Just Accepted” as a service to the research community to expedite the dissemination of scientific material as soon as possible after acceptance. “Just Accepted” manuscripts appear in full in PDF format accompanied by an HTML abstract. “Just Accepted” manuscripts have been fully peer reviewed, but should not be considered the official version of record. They are citable by the Digital Object Identifier (DOI®). “Just Accepted” is an optional service offered to authors. Therefore, the “Just Accepted” Web site may not include all articles that will be published in the journal. After a manuscript is technically edited and formatted, it will be removed from the “Just Accepted” Web site and published as an ASAP article. Note that technical editing may introduce minor changes to the manuscript text and/or graphics which could affect content, and all legal disclaimers and ethical guidelines that apply to the journal pertain. ACS cannot be held responsible for errors or consequences arising from the use of information contained in these “Just Accepted” manuscripts.

1  
2  
3  
4  
5  
6  
7  
8  
9  
10  
11  
12  
13  
14  
15  
16  
17  
18  
19  
20  
21  
22  
23  
24  
25  
26  
27  
28  
29  
30  
31  
32  
33  
34  
35  
36  
37  
38  
39  
40  
41  
42  
43  
44  
45  
46  
47  
48  
49  
50  
51  
52  
53  
54  
55  
56  
57  
58  
59  
60

# COSMO<sub>perm</sub>: Mechanistic Prediction of Passive Membrane Permeability for Neutral Compounds and Ions, and its pH Dependence

*Johannes A. H. Schwöbel*<sup>1,\*</sup>, *Andrea Ebert*<sup>2,3</sup>, *Kai Bittermann*<sup>2</sup>, *Uwe Huniar*<sup>1</sup>, *Kai-Uwe Goss*<sup>2,4</sup>,  
*Andreas Klamt*<sup>1,5</sup>

<sup>1</sup> BIOVIA, Dassault Systèmes Deutschland GmbH, Imbacher Weg 46, D-51379 Leverkusen, Germany

<sup>2</sup> UFZ - Helmholtz Centre for Environmental Research, Permoserstraße 15, D-04318 Leipzig, Germany

<sup>3</sup> Institute of Biophysics, Johannes Kepler University, Gruberstraße 40, 4020 Linz, Austria

<sup>4</sup> Institute of Chemistry, University of Halle-Wittenberg, Kurt Mothes Str. 2, D-06120 Halle, Germany

<sup>5</sup> University of Regensburg, Universitätsstraße 31, D-93053 Regensburg, Germany

1  
2  
3 ABSTRACT  
4  
5  
6  
7

8 We present the new and entirely mechanistic *COSMOperm* method to predict passive membrane  
9 permeabilities for neutral compounds, as well as anions and cations. The *COSMOperm* approach  
10 is based on compound specific free energy profiles within a membrane of interest from COSMO-  
11 RS (Conductor-like Screening Model for Realistic Solvation) calculations. These are combined  
12 with membrane layer-specific diffusion coefficients, for example, in the water phase, the polar  
13 head groups and the alkyl tails of biochemical phospholipid bilayers. COSMO-RS utilizes first-  
14 principle quantum chemical structures and physically sound intermolecular interactions  
15 (electrostatic, hydrogen bond and van der Waals). For this reason, it is unbiased towards different  
16 application scenarios, such as cosmetics, industrial chemical or pharmaceutical industries. A fully  
17 predictive calculation of passive permeation through phospholipid bilayer membranes results in a  
18 performance of  $r^2 = 0.92$ ;  $rmsd = 0.90 \log_{10}$  units for neutral compounds and anions, as compared  
19 to gold standard black lipid membrane (BLM) experiments. It will be demonstrated that new  
20 membrane types can be generated by the related *COSMOplex* method and directly used for  
21 permeability studies by *COSMOperm*.  
22  
23  
24  
25  
26  
27  
28  
29  
30  
31  
32  
33  
34  
35  
36  
37  
38  
39  
40  
41  
42  
43  
44  
45  
46  
47  
48  
49  
50  
51  
52  
53  
54  
55  
56  
57  
58  
59  
60

1  
2  
3 INTRODUCTION  
4  
5  
6  
7

8 Biomembrane permeabilities are of general interest in the uptake and distribution of  
9 pharmaceutical agents, chemical toxicants and environmental pollutants. Small solutes can  
10 permeate the phospholipid membrane by a passive diffusion process, and driven by a concentration  
11 gradient between the aqueous regions at the two sides of a bilayer.<sup>1,2</sup>  
12  
13  
14

15 The intrinsic permeability coefficient  $P$  is defined from the steady-state-flux  $J_{ss} = -P \Delta c$  across  
16 the phospholipid bilayer with a particular concentration difference  $\Delta c$ . Transport of small solutes  
17 can be described by Overton's rule and a more quantitative approach which is known as the  
18 solubility-diffusion model.<sup>2,3</sup>  
19  
20  
21  
22  
23  
24  
25

26 In Overton's concept, the phospholipid membrane is regarded as a homogeneous organic matrix  
27 acting as barrier for solute diffusion. According to this, solutes transfer from water to the  
28 membrane with a volume based partition coefficient  $K = c_m / c_w$  with  $c_m$  being the concentration  
29 in the membrane and  $c_w$  the concentration in water, both in in mol/l units). Fick's first law can be  
30 formulated as the following expression, with a phospholipid bilayer thickness of  $2L$  and a  
31 concentration difference  $\Delta c_m$  within the membrane phase, or  $\Delta c_w$  between the aqueous donor and  
32 acceptor compartments of a permeability system:  
33  
34  
35  
36  
37  
38  
39  
40  
41  
42  
43  
44

$$45 J_{SS} = -\frac{D}{2L}\Delta c_m = -\frac{D}{2L}K\Delta c_w \quad (1)$$

46  
47  
48  
49

50 Thus, leading to the simplified expression:  
51  
52  
53  
54

$$55 P = \frac{DK}{2L} \quad (2)$$

56  
57  
58  
59  
60

1  
2  
3  
4  
5  
6 However, permeability through the membrane is dominated by those parts that are the least  
7 attractive and thus impose a free energy barrier. It is therefore no surprise that pure membrane  
8 permeability does not correlate well with membrane partition coefficients;<sup>3</sup> even though it is quite  
9 often correlated with partition coefficients to bulk solvents (e.g., 1-octanol to water or 1,9-  
10 decanediene to water).<sup>4</sup> For this reason, existing models for membrane permeation use alkane  
11 solvents such as hexadecane as a surrogate to mimic the membrane core, which is supposed to be  
12 the main barrier in membrane permeation for most compounds.<sup>3,5</sup> However, the bilayer  
13 environment is highly anisotropic along the normal direction  $\vec{z}$  to the membrane surface.<sup>6</sup> An  
14 inhomogeneous solubility-diffusion model was proposed by Diamond and Katz in 1974,<sup>7</sup> arriving  
15 at the following analytical expression for the steady-state-flux of solutes through a membrane:  
16  
17  
18  
19  
20  
21  
22  
23  
24  
25  
26  
27  
28  
29  
30

$$J_{SS} = - \frac{c(L) - c(-L)}{\int_{-L}^L \left[ \frac{1}{K(z)D(z)} \right] dz} \quad (3)$$

$$\frac{1}{P} = \int_{-L}^L \left[ \frac{1}{K(z)D(z)} \right] dz \quad (4)$$

31  
32  
33  
34  
35  
36  
37  
38  
39  
40 Here,  $K(z)$  and  $D(z)$  are local partition and diffusion coefficients, respectively, at the solute position  
41  $z$  (with  $z = 0$  being the center of a bilayer membrane and  $z = \pm L$  the boundaries of the symmetrical  
42 membrane). The solute position can be, e.g., in the aqueous phase, the polar head groups or the  
43 alkyl tails of biochemical phospholipid bilayers. The **equation 4** assumes that the diffusion in the  
44 membrane interior can be described by the Nernst-Planck equation in the absence of activated  
45 processes.<sup>6</sup> Indeed, missing a systematic derivation in literature, we counterchecked these  
46  
47  
48  
49  
50  
51  
52  
53  
54  
55  
56  
57  
58  
59  
60

1  
2  
3 equations and came to the conclusion that the Diamond-Katz model is in exact agreement with  
4  
5 Fick's laws of diffusion, as long as local diffusion and partition coefficients can be defined.  
6  
7  
8  
9

10 The local partition and diffusion coefficients are not experimentally accessible. Typically, they are  
11 predicted using time-consuming molecular dynamics (MD) simulations, partially relying on  
12 supercomputing facilities; a few examples are listed in the references.<sup>1,6,8,9</sup> As an alternative, we  
13 present the new and entirely mechanistic *COSMOperm* method to predict passive membrane  
14 permeabilities. The *COSMOperm* approach is based on compound specific free energy profiles  
15  $\Delta G(z)$  within a biomembrane of interest from COSMO-RS (Conductor-like Screening Model for  
16 Realistic Solvation) calculations.<sup>10,11</sup> These free energy profiles are computed by the *COSMOmic*  
17 method,<sup>12</sup> which has been demonstrated to yield at least comparably reliable results for the free  
18 energies of neutral solutes in micellar systems as achievable with MD simulations; but at about  
19 0.01 percent of the computational cost (i.e., typically within a few minutes on a standard laptop  
20 computer with available quantum chemical COSMO information).<sup>13-15</sup> The local free energies are  
21 complemented by membrane layer specific diffusion coefficients  $D(z)$ , again, applying COSMO-  
22 RS parameters.  
23  
24  
25  
26  
27  
28  
29  
30  
31  
32  
33  
34  
35  
36  
37  
38  
39  
40  
41

42 COSMO-RS utilizes first-principle quantum chemical structures and physically sound  
43 intermolecular interactions (electrostatic, hydrogen bond and van der Waals), and the  
44 *COSMOperm* method is designed to predict the membrane permeability not only of neutral, but  
45 also of charged compounds right from the beginning. While there already exist different models  
46 to predict the permeability of neutral compounds,<sup>3,5,16</sup> to the best of our knowledge, there are no  
47 alternative systematical methods capable of predicting permeation rates of anions and cations.  
48  
49  
50  
51  
52  
53  
54  
55  
56  
57  
58  
59  
60

1  
2  
3 Nevertheless, the permeation of charged compounds is of potential interest for the biophysical  
4 research of fatty acid anions,<sup>5</sup> uncouplers of phosphorylation,<sup>17</sup> antibiotics,<sup>18</sup> drugs,<sup>19</sup> and  
5  
6 nutrients.<sup>20</sup> In addition, the COSMO $perm$  model is not limited to specific membrane types, but any  
7  
8 atomistic membrane structure at the liquid-crystalline state generated by the COSMO $plex$  method  
9  
10 can be applied.<sup>21</sup> COSMO $perm$  can be seen as a further development of the COSMO $mic$  method  
11  
12 mentioned above. COSMO $mic$  originally was only applicable for neutral compounds and has itself  
13  
14 been extended to ionic solutes before, allowing for the prediction of membrane to water partition  
15  
16 coefficients of neutral and ionic species with an accuracy of about 0.7 log<sub>10</sub> units.<sup>22,23</sup> the correct  
17  
18 physical treatment of the energy barrier of ions in the alkyl phase (i.e., the center of a bilayer  
19  
20 membrane) has been handled by the Born energy contribution.  
21  
22  
23  
24  
25  
26  
27

28 In this paper, the COSMO $perm$  model is validated against experimental black lipid membrane  
29  
30 (BLM) permeabilities, for neutral compounds, ionizable compounds and permanent ions. BLM  
31  
32 experiments are considered as gold standard for determining permeability values, because they are  
33  
34 free of artifacts that may accompany cell-line experiments such as metabolism, active transport or  
35  
36 ion-trapping in lysosomes.<sup>3</sup>  
37  
38  
39  
40  
41

## 42 MATERIALS AND METHODS

43  
44  
45  
46

47 **Experimental BLM Data.** Black lipid membrane (BLM) permeability data are collected  
48  
49 from the literature. The validation data compilation includes neutral compounds as well as ionic  
50  
51 protonation states and permanent ions.  
52  
53  
54  
55  
56  
57  
58  
59  
60

1  
2  
3 In short, two compartments of a Teflon chamber are separated by a septum in a BLM experiment.  
4  
5 A planar lipid bilayer of a few nanometers in size is formed across a small hole (about 100  $\mu\text{m}$  to  
6  
7 1.5 mm in diameter) in the septum, which is pre-coated by hexadecane or by phospholipids  
8  
9 dissolved in hydrophobic, viscous solvents (e.g., decane).<sup>24,25</sup> Both compartments are filled by  
10  
11 aqueous buffer solution maintaining the pH value of particular interest and are magnetically  
12  
13 stirred. The two BLM compartments are accessible electrodes are placed into both compartments  
14  
15 and voltage or chemical gradients are applied. This allows to measure conductivities of ions or of  
16  
17 the corresponding pH dependence of conductivities at electrophysiological conditions. Analytical,  
18  
19 chemical or radiotracer methods may determine fluxes along an applied chemical gradient for  
20  
21 neutral compounds. For fast permeating compounds, special care has to be taken to avoid limiting  
22  
23 effects due to the aqueous boundary layer and associated acid-base reactions.<sup>26,27</sup> More details are  
24  
25 presented by the workgroups of Gutknecht *et al.*,<sup>28</sup> Xiang *et al.*,<sup>29</sup> and Pohl *et al.*,<sup>30,31</sup>  
26  
27  
28  
29  
30

31 The dataset is shown in **Table 1**. The experimental sources for neutral compounds, anions and  
32  
33 cations are listed in the table. If more than one experimental value was reported in the literature  
34  
35 for the same compound, the value derived from the membrane type closest to the DMPC (1,2-  
36  
37 dimyristoyl-*sn*-glycero-3-phosphocholine) reference was taken.  
38  
39  
40  
41  
42  
43

44 **COSMO-RS.** The conductor-like screening model for realistic solvation (COSMO-RS) is  
45  
46 a combination of the dielectric continuum solvation model COSMO<sup>32</sup> with an efficient statistical  
47  
48 thermodynamic model of pairwise molecular surface interactions,<sup>10,11</sup> using the surface  
49  
50 polarization charge densities  $\sigma$  of solutes and solvents arising from quantum chemical COSMO  
51  
52 calculations. As most important molecular interaction modes, electrostatics and hydrogen bonding  
53  
54  
55  
56  
57  
58  
59  
60

1  
2  
3 are considered. The less specific dispersive interactions are described to first order based on  
4  
5 element specific surface energies.<sup>33</sup>  
6  
7  
8  
9

10 **COSMOmic.** The *COSMOmic* extension for inhomogeneous systems uses information about  
11 the structure of a membrane. The membrane structure is represented by a layered liquid system of  
12 varying composition per layer with respect to the COSMO polarization charge density  
13 distributions, i.e., the so-called  $\sigma$ -profiles.<sup>12</sup> The generation of the membrane structures is  
14 described in the next section.  
15  
16  
17  
18  
19

20  
21 *COSMOmic* calculates the free energies of solutes in such a layered liquid system by sampling  
22 over all relevant positions, orientations and conformations of the solute in this system, resulting in  
23 reliable predictions of membrane to water partition coefficients and free energy profiles of solutes.  
24 Herein, the orientations are provided by rotations around the polarity-based center of the  
25 compound, because as a side-condition the polar sites need to cross all parts of the membrane as  
26 part of the permeation process. No additional side-conditions are introduced (e.g., to prevent flip-  
27 flops): the compounds are allowed to occupy all thermodynamically reasonable rotational states,  
28 by default the rotational states are defined by a set of 162 orientations per conformer and layer.  
29 The local membrane to water partition coefficient  $K(z)$  is in thermodynamic relationship to the  
30 spatial free energy  $\Delta G_{\text{mic}}(z)$ , as calculated by *COSMOmic* by the sampling mentioned above:  
31  
32  
33  
34  
35  
36  
37  
38  
39  
40  
41  
42  
43  
44  
45  
46

$$47 \quad K(z) = \exp\left(\frac{-\Delta G_{\text{mic}}(z)}{RT}\right) \quad (5)$$

48  
49  
50  
51

52 *COSMOmic* has a proven track to provide at least comparably reliable results for the free energies  
53 of neutral solutes in micellar systems as achievable with MD simulations, at a fraction of the  
54  
55  
56  
57  
58  
59  
60

1  
2  
3 computational cost.<sup>34</sup> More recently, *COSMOmic* has been extended to ionic solutes, now allowing  
4 the prediction of the phospholipid membrane to water partition coefficients of neutral and ionic  
5 species with an accuracy of about  $0.7 \log_{10}$  units.<sup>22,23</sup> No special parameterization of *COSMOmic*  
6 was required beyond the underlying COSMO-RS parameterization. Only for inclusion of ions, the  
7 membrane dipole potential<sup>35</sup> needed to be derived from fitting of an appropriate functional form  
8 with three adjustable parameters.  
9  
10  
11  
12  
13  
14  
15  
16  
17  
18

19 **Virtual Membranes Systems.** Two virtual membrane structures are used within this work  
20 and compared to each other.  
21  
22

23 The first membrane structure is taken from atomic distributions of molecular dynamics (MD)  
24 simulations. Herein, time-averaged atomic distributions of a classic phospholipid system (1,2-  
25 dimyristoyl-*sn*-glycero-3-phosphocholine, abbreviated as DMPC) were kindly simulated  
26 (CHARMM36 force field) and provided by Jakobtorweihen.<sup>34</sup> A DMPC membrane potential is  
27 applied, where three adjustable parameters per computational level are fitted for an optimal  
28 prediction of membrane to water partition coefficients.  
29  
30  
31  
32  
33  
34  
35  
36

37 The second structure is generated by a self-consistent and iterative variant of *COSMOmic*, called  
38 *COSMOplex*. This novel method can simulate the self-organization of micelles and membrane  
39 structures as a fast alternative to MD simulations, typically in only 0.01% of the computational  
40 time. For details of the *COSMOplex* method, the reader is referred to the publication of Klamt *et*  
41 *al.*<sup>21</sup> In this study, the *COSMOplex* method is used to generate artificial chlorodecane containing  
42 phospholipid bilayers as an occasionally used experimental reference system for mitochondrial  
43 membranes.<sup>36</sup> They show an increased permeability, as compared to classic phospholipid  
44 membranes. The *COSMOplex* system is set up by using two conformer sets, DMPC and  
45  
46  
47  
48  
49  
50  
51  
52  
53  
54  
55  
56  
57  
58  
59  
60

1  
2  
3 chlorodecane, plus water; more in detail, making use of the “autobox” functionality of the  
4 COSMOplex software with standard parameters and activated segment directionality (DIRPLEX)  
5  
6  
7 to arrive at a reasonable initial guess for the membrane system. The converged layered membrane  
8  
9  
10 system is used as input for further COSMOperm calculations. In this COSMOplex membrane the  
11  
12 scaled membrane potential of the chlorodecane/DMPC system is generated in a self-consistent  
13  
14 way by COSMOplex.

15  
16  
17 More details on the membrane structures and the membrane potentials are listed in section S3 of  
18  
19 the supporting information.  
20  
21  
22  
23

24 **Permeability in Inhomogeneous Membranes.** The permeability  $P$  is calculated according  
25  
26 to the inhomogeneous solubility-diffusion model, which was deduced in very detail by Diamond  
27  
28 and Katz, see **equation 4**.<sup>7</sup> The following initial equations assume a single compound or  
29  
30 protonation state penetrating the membrane. In this case, the resistance  $R(z) = 1/P(z)$  in a particular  
31  
32 penetration depth  $z$  is defined in the following way:  
33  
34  
35  
36  
37

$$R(z) = \frac{dz}{K(z)D(z)} \quad (6)$$

38  
39  
40  
41  
42 In this equation,  $K(z)$  is the local membrane/water partition coefficient in [(mol/l)/(mol/l)],  
43  
44 calculated by **equation 5**;  $D(z)$  the local diffusion coefficient of solutes penetrating a membrane  
45  
46 layer, typically in [m<sup>2</sup>/s]; and  $dz$  is the depth of a membrane layer in [m]. The overall steady-state  
47  
48 permeability  $P$  is then calculated:  
49  
50  
51  
52  
53

$$P_{\text{steady - state}} = \frac{1}{\sum_{\text{layers}} R(z)} \quad (7)$$

1  
2  
3  
4  
5  
6       **Prediction of Diffusion Coefficients.** The missing link between the chemical potential  
7 provided by COSMOmic in **equation 5** and the kinetics in **equation 6** are the layer-specific  
8 diffusion coefficients  $D(z)$ . Briefly, they are calculated via COSMO-RS based parameters from  
9 entropic and enthalpic contributions of solute-solvent and solvent-solvent interactions. Here, the  
10 solute is the permeating molecular species and the solvent environment a particular membrane  
11 layer of depth  $z$ . The layer-specific diffusion coefficient prediction is completed by the COSMO  
12 surface area of the permeant, as the magnitude of the shear force is proportional to the area, and a  
13 temperature dependence according to the Stokes-Einstein hydrodynamic theory.<sup>37</sup> The diffusion  
14 model is fitted against bulk liquid diffusion coefficients collected from the literature ( $n = 499$ ;  $r^2$   
15  $= 0.81$ ;  $rmsd = 0.298$  ln units;  $F = 447$ ), and used in a fully predictive manner within COSMOperm.  
16 More details are shown in section S1 of the supporting information.

17  
18  
19  
20  
21  
22  
23  
24  
25  
26  
27  
28  
29  
30  
31  
32  
33  
34  
35  
36  
37  
38  
39  
40  
41  
42  
43  
44  
45  
46  
47  
48  
49  
50  
51  
52  
53  
54  
55  
56  
57  
58  
59  
60  
In principle, the COSMOperm model is independent from the underlying diffusion model used,  
and more mechanistic diffusion models might replace this semi-empirical model in the future.

61  
62  
63  
64  
65  
66  
67  
68  
69  
70  
71  
72  
73  
74  
75  
76  
77  
78  
79  
80  
81  
82  
83  
84  
85  
86  
87  
88  
89  
90  
91  
92  
93  
94  
95  
96  
97  
98  
99  
100  
**pH Dependent Protonation States.** A search of the World Drug Index for 1999 suggested  
that 63 % of the listed drugs were ionizable. Therefore, the consideration of protonation states is  
one important aspect for the quantification of membrane permeation.

101  
102  
103  
104  
105  
106  
107  
108  
109  
110  
111  
112  
113  
114  
115  
116  
117  
118  
119  
120  
121  
122  
123  
124  
125  
126  
127  
128  
129  
130  
131  
132  
133  
134  
135  
136  
137  
138  
139  
140  
141  
142  
143  
144  
145  
146  
147  
148  
149  
150  
151  
152  
153  
154  
155  
156  
157  
158  
159  
160  
161  
162  
163  
164  
165  
166  
167  
168  
169  
170  
171  
172  
173  
174  
175  
176  
177  
178  
179  
180  
181  
182  
183  
184  
185  
186  
187  
188  
189  
190  
191  
192  
193  
194  
195  
196  
197  
198  
199  
200  
201  
202  
203  
204  
205  
206  
207  
208  
209  
210  
211  
212  
213  
214  
215  
216  
217  
218  
219  
220  
221  
222  
223  
224  
225  
226  
227  
228  
229  
230  
231  
232  
233  
234  
235  
236  
237  
238  
239  
240  
241  
242  
243  
244  
245  
246  
247  
248  
249  
250  
251  
252  
253  
254  
255  
256  
257  
258  
259  
260  
261  
262  
263  
264  
265  
266  
267  
268  
269  
270  
271  
272  
273  
274  
275  
276  
277  
278  
279  
280  
281  
282  
283  
284  
285  
286  
287  
288  
289  
290  
291  
292  
293  
294  
295  
296  
297  
298  
299  
300  
301  
302  
303  
304  
305  
306  
307  
308  
309  
310  
311  
312  
313  
314  
315  
316  
317  
318  
319  
320  
321  
322  
323  
324  
325  
326  
327  
328  
329  
330  
331  
332  
333  
334  
335  
336  
337  
338  
339  
340  
341  
342  
343  
344  
345  
346  
347  
348  
349  
350  
351  
352  
353  
354  
355  
356  
357  
358  
359  
360  
361  
362  
363  
364  
365  
366  
367  
368  
369  
370  
371  
372  
373  
374  
375  
376  
377  
378  
379  
380  
381  
382  
383  
384  
385  
386  
387  
388  
389  
390  
391  
392  
393  
394  
395  
396  
397  
398  
399  
400  
401  
402  
403  
404  
405  
406  
407  
408  
409  
410  
411  
412  
413  
414  
415  
416  
417  
418  
419  
420  
421  
422  
423  
424  
425  
426  
427  
428  
429  
430  
431  
432  
433  
434  
435  
436  
437  
438  
439  
440  
441  
442  
443  
444  
445  
446  
447  
448  
449  
450  
451  
452  
453  
454  
455  
456  
457  
458  
459  
460  
461  
462  
463  
464  
465  
466  
467  
468  
469  
470  
471  
472  
473  
474  
475  
476  
477  
478  
479  
480  
481  
482  
483  
484  
485  
486  
487  
488  
489  
490  
491  
492  
493  
494  
495  
496  
497  
498  
499  
500  
501  
502  
503  
504  
505  
506  
507  
508  
509  
510  
511  
512  
513  
514  
515  
516  
517  
518  
519  
520  
521  
522  
523  
524  
525  
526  
527  
528  
529  
530  
531  
532  
533  
534  
535  
536  
537  
538  
539  
540  
541  
542  
543  
544  
545  
546  
547  
548  
549  
550  
551  
552  
553  
554  
555  
556  
557  
558  
559  
560  
561  
562  
563  
564  
565  
566  
567  
568  
569  
570  
571  
572  
573  
574  
575  
576  
577  
578  
579  
580  
581  
582  
583  
584  
585  
586  
587  
588  
589  
590  
591  
592  
593  
594  
595  
596  
597  
598  
599  
600  
601  
602  
603  
604  
605  
606  
607  
608  
609  
610  
611  
612  
613  
614  
615  
616  
617  
618  
619  
620  
621  
622  
623  
624  
625  
626  
627  
628  
629  
630  
631  
632  
633  
634  
635  
636  
637  
638  
639  
640  
641  
642  
643  
644  
645  
646  
647  
648  
649  
650  
651  
652  
653  
654  
655  
656  
657  
658  
659  
660  
661  
662  
663  
664  
665  
666  
667  
668  
669  
670  
671  
672  
673  
674  
675  
676  
677  
678  
679  
680  
681  
682  
683  
684  
685  
686  
687  
688  
689  
690  
691  
692  
693  
694  
695  
696  
697  
698  
699  
700  
701  
702  
703  
704  
705  
706  
707  
708  
709  
710  
711  
712  
713  
714  
715  
716  
717  
718  
719  
720  
721  
722  
723  
724  
725  
726  
727  
728  
729  
730  
731  
732  
733  
734  
735  
736  
737  
738  
739  
740  
741  
742  
743  
744  
745  
746  
747  
748  
749  
750  
751  
752  
753  
754  
755  
756  
757  
758  
759  
760  
761  
762  
763  
764  
765  
766  
767  
768  
769  
770  
771  
772  
773  
774  
775  
776  
777  
778  
779  
780  
781  
782  
783  
784  
785  
786  
787  
788  
789  
790  
791  
792  
793  
794  
795  
796  
797  
798  
799  
800  
801  
802  
803  
804  
805  
806  
807  
808  
809  
810  
811  
812  
813  
814  
815  
816  
817  
818  
819  
820  
821  
822  
823  
824  
825  
826  
827  
828  
829  
830  
831  
832  
833  
834  
835  
836  
837  
838  
839  
840  
841  
842  
843  
844  
845  
846  
847  
848  
849  
850  
851  
852  
853  
854  
855  
856  
857  
858  
859  
860  
861  
862  
863  
864  
865  
866  
867  
868  
869  
870  
871  
872  
873  
874  
875  
876  
877  
878  
879  
880  
881  
882  
883  
884  
885  
886  
887  
888  
889  
890  
891  
892  
893  
894  
895  
896  
897  
898  
899  
900  
901  
902  
903  
904  
905  
906  
907  
908  
909  
910  
911  
912  
913  
914  
915  
916  
917  
918  
919  
920  
921  
922  
923  
924  
925  
926  
927  
928  
929  
930  
931  
932  
933  
934  
935  
936  
937  
938  
939  
940  
941  
942  
943  
944  
945  
946  
947  
948  
949  
950  
951  
952  
953  
954  
955  
956  
957  
958  
959  
960  
961  
962  
963  
964  
965  
966  
967  
968  
969  
970  
971  
972  
973  
974  
975  
976  
977  
978  
979  
980  
981  
982  
983  
984  
985  
986  
987  
988  
989  
990  
991  
992  
993  
994  
995  
996  
997  
998  
999  
1000  
1001  
1002  
1003  
1004  
1005  
1006  
1007  
1008  
1009  
1010  
1011  
1012  
1013  
1014  
1015  
1016  
1017  
1018  
1019  
1020  
1021  
1022  
1023  
1024  
1025  
1026  
1027  
1028  
1029  
1030  
1031  
1032  
1033  
1034  
1035  
1036  
1037  
1038  
1039  
1040  
1041  
1042  
1043  
1044  
1045  
1046  
1047  
1048  
1049  
1050  
1051  
1052  
1053  
1054  
1055  
1056  
1057  
1058  
1059  
1060  
1061  
1062  
1063  
1064  
1065  
1066  
1067  
1068  
1069  
1070  
1071  
1072  
1073  
1074  
1075  
1076  
1077  
1078  
1079  
1080  
1081  
1082  
1083  
1084  
1085  
1086  
1087  
1088  
1089  
1090  
1091  
1092  
1093  
1094  
1095  
1096  
1097  
1098  
1099  
1100  
1101  
1102  
1103  
1104  
1105  
1106  
1107  
1108  
1109  
1110  
1111  
1112  
1113  
1114  
1115  
1116  
1117  
1118  
1119  
1120  
1121  
1122  
1123  
1124  
1125  
1126  
1127  
1128  
1129  
1130  
1131  
1132  
1133  
1134  
1135  
1136  
1137  
1138  
1139  
1140  
1141  
1142  
1143  
1144  
1145  
1146  
1147  
1148  
1149  
1150  
1151  
1152  
1153  
1154  
1155  
1156  
1157  
1158  
1159  
1160  
1161  
1162  
1163  
1164  
1165  
1166  
1167  
1168  
1169  
1170  
1171  
1172  
1173  
1174  
1175  
1176  
1177  
1178  
1179  
1180  
1181  
1182  
1183  
1184  
1185  
1186  
1187  
1188  
1189  
1190  
1191  
1192  
1193  
1194  
1195  
1196  
1197  
1198  
1199  
1200  
1201  
1202  
1203  
1204  
1205  
1206  
1207  
1208  
1209  
1210  
1211  
1212  
1213  
1214  
1215  
1216  
1217  
1218  
1219  
1220  
1221  
1222  
1223  
1224  
1225  
1226  
1227  
1228  
1229  
1230  
1231  
1232  
1233  
1234  
1235  
1236  
1237  
1238  
1239  
1240  
1241  
1242  
1243  
1244  
1245  
1246  
1247  
1248  
1249  
1250  
1251  
1252  
1253  
1254  
1255  
1256  
1257  
1258  
1259  
1260  
1261  
1262  
1263  
1264  
1265  
1266  
1267  
1268  
1269  
1270  
1271  
1272  
1273  
1274  
1275  
1276  
1277  
1278  
1279  
1280  
1281  
1282  
1283  
1284  
1285  
1286  
1287  
1288  
1289  
1290  
1291  
1292  
1293  
1294  
1295  
1296  
1297  
1298  
1299  
1300  
1301  
1302  
1303  
1304  
1305  
1306  
1307  
1308  
1309  
1310  
1311  
1312  
1313  
1314  
1315  
1316  
1317  
1318  
1319  
1320  
1321  
1322  
1323  
1324  
1325  
1326  
1327  
1328  
1329  
1330  
1331  
1332  
1333  
1334  
1335  
1336  
1337  
1338  
1339  
1340  
1341  
1342  
1343  
1344  
1345  
1346  
1347  
1348  
1349  
1350  
1351  
1352  
1353  
1354  
1355  
1356  
1357  
1358  
1359  
1360  
1361  
1362  
1363  
1364  
1365  
1366  
1367  
1368  
1369  
1370  
1371  
1372  
1373  
1374  
1375  
1376  
1377  
1378  
1379  
1380  
1381  
1382  
1383  
1384  
1385  
1386  
1387  
1388  
1389  
1390  
1391  
1392  
1393  
1394  
1395  
1396  
1397  
1398  
1399  
1400  
1401  
1402  
1403  
1404  
1405  
1406  
1407  
1408  
1409  
1410  
1411  
1412  
1413  
1414  
1415  
1416  
1417  
1418  
1419  
1420  
1421  
1422  
1423  
1424  
1425  
1426  
1427  
1428  
1429  
1430  
1431  
1432  
1433  
1434  
1435  
1436  
1437  
1438  
1439  
1440  
1441  
1442  
1443  
1444  
1445  
1446  
1447  
1448  
1449  
1450  
1451  
1452  
1453  
1454  
1455  
1456  
1457  
1458  
1459  
1460  
1461  
1462  
1463  
1464  
1465  
1466  
1467  
1468  
1469  
1470  
1471  
1472  
1473  
1474  
1475  
1476  
1477  
1478  
1479  
1480  
1481  
1482  
1483  
1484  
1485  
1486  
1487  
1488  
1489  
1490  
1491  
1492  
1493  
1494  
1495  
1496  
1497  
1498  
1499  
1500  
1501  
1502  
1503  
1504  
1505  
1506  
1507  
1508  
1509  
1510  
1511  
1512  
1513  
1514  
1515  
1516  
1517  
1518  
1519  
1520  
1521  
1522  
1523  
1524  
1525  
1526  
1527  
1528  
1529  
1530  
1531  
1532  
1533  
1534  
1535  
1536  
1537  
1538  
1539  
1540  
1541  
1542  
1543  
1544  
1545  
1546  
1547  
1548  
1549  
1550  
1551  
1552  
1553  
1554  
1555  
1556  
1557  
1558  
1559  
1560  
1561  
1562  
1563  
1564  
1565  
1566  
1567  
1568  
1569  
1570  
1571  
1572  
1573  
1574  
1575  
1576  
1577  
1578  
1579  
1580  
1581  
1582  
1583  
1584  
1585  
1586  
1587  
1588  
1589  
1590  
1591  
1592  
1593  
1594  
1595  
1596  
1597  
1598  
1599  
1600  
1601  
1602  
1603  
1604  
1605  
1606  
1607  
1608  
1609  
1610  
1611  
1612  
1613  
1614  
1615  
1616  
1617  
1618  
1619  
1620  
1621  
1622  
1623  
1624  
1625  
1626  
1627  
1628  
1629  
1630  
1631  
1632  
1633  
1634  
1635  
1636  
1637  
1638  
1639  
1640  
1641  
1642  
1643  
1644  
1645  
1646  
1647  
1648  
1649  
1650  
1651  
1652  
1653  
1654  
1655  
1656  
1657  
1658  
1659  
1660  
1661  
1662  
1663  
1664  
1665  
1666  
1667  
1668  
1669  
1670  
1671  
1672  
1673  
1674  
1675  
1676  
1677  
1678  
1679  
1680  
1681  
1682  
1683  
1684  
1685  
1686  
1687  
1688  
1689  
1690  
1691  
1692  
1693  
1694  
1695  
1696  
1697  
1698  
1699  
1700  
1701  
1702  
1703  
1704  
1705  
1706  
1707  
1708  
1709  
1710  
1711  
1712  
1713  
1714  
1715  
1716  
1717  
1718  
1719  
1720  
1721  
1722  
1723  
1724  
1725  
1726  
1727  
1728  
1729  
1730  
1731  
1732  
1733  
1734  
1735  
1736  
1737  
1738  
1739  
1740  
1741  
1742  
1743  
1744  
1745  
1746  
1747  
1748  
1749  
1750  
1751  
1752  
1753  
1754  
1755  
1756  
1757  
1758  
1759  
1760  
1761  
1762  
1763  
1764  
1765  
1766  
1767  
1768  
1769  
1770  
1771  
1772  
1773  
1774  
1775  
1776  
1777  
1778  
1779  
1780  
1781  
1782  
1783  
1784  
1785  
1786  
1787  
1788  
1789  
1790  
1791  
1792  
1793  
1794  
1795  
1796  
1797  
1798  
1799  
1800  
1801  
1802  
1803  
1804  
1805  
1806  
1807  
1808  
1809  
1810  
1811  
1812  
1813  
1814  
1815  
1816  
1817  
1818  
1819  
1820  
1821  
1822  
1823  
1824  
1825  
1826  
1827  
1828  
1829  
1830  
1831  
1832  
1833  
1834  
1835  
1836  
1837  
1838  
1839  
1840  
1841  
1842  
1843  
1844  
1845  
1846  
1847  
1848  
1849  
1850  
1851  
1852  
1853  
1854  
1855  
1856  
1857  
1858  
1859  
1860  
1861  
1862  
1863  
1864  
1865  
1866  
1867  
1868  
1869  
1870  
1871  
1872  
1873  
1874  
1875  
1876  
1877  
1878  
1879  
1880  
1881  
1882  
1883  
1884  
1885  
1886  
1887  
1888  
1889  
1890  
1891  
1892  
1893  
1894  
1895  
1896  
1897  
1898  
1899  
1900  
1901  
1902  
1903  
1904  
1905  
1906  
1907  
1908  
1909  
1910  
1911  
1912  
1913  
1914  
1915  
1916  
1917  
1918  
1919  
1920  
1921  
1922  
1923  
1924  
1925  
1926  
1927  
1928  
1929  
1930  
1931  
1932  
1933  
1934  
1935  
1936  
1937  
1938  
1939  
1940  
1941  
1942  
1943  
1944  
1945  
1946  
1947  
1948  
1949  
1950  
1951  
1952  
1953  
1954  
1955  
1956  
1957  
1958  
1959  
1960  
1961  
1962  
1963  
1964  
1965  
1966  
1967  
1968  
1969  
1970  
1971  
1972  
1973  
1974  
1975  
1976  
1977  
1978  
1979  
1980  
1981  
1982  
1983  
1984  
1985  
1986  
1987  
1988  
1989  
1990  
1991  
1992  
1993  
1994  
1995  
1996  
1997  
1998  
1999  
2000  
2001  
2002  
2003  
2004  
2005  
2006  
2007  
2008  
2009  
2010  
2011  
2012  
2013  
2014  
2015  
2016  
2017  
2018  
2019  
2020  
2021  
2022  
2023  
2024  
2025  
2026  
2027  
2028  
2029  
2030  
2031  
2032  
2033  
2034  
2035  
2036  
2037  
2038  
2039  
2040  
2041  
2042  
2043  
2044  
2045  
2046  
2047  
2048  
2049  
2050  
2051  
2052  
2053  
2054  
2055  
2056  
2057  
2058  
2059  
2060  
2061  
2062  
2063  
2064  
2065  
2066  
2067  
2068  
2069  
2070  
2071  
2072  
2073  
2074  
2075  
2076  
2077  
2078  
2079  
2080  
2081  
2082  
2083  
2084  
2085  
2086  
2087  
2088  
2089  
2090  
2091  
2092  
2093  
2094  
2095  
2096  
2097  
2098  
2099  
2100  
2101  
2102  
2103  
2104  
2105  
2106  
2107  
2108  
2109  
2110  
2111  
2112  
2113  
2114  
2115  
2116  
2117  
2118  
2119  
2120  
2121  
2122  
2123  
2124  
2125  
2126  
2127  
2128  
2129  
2130  
2131  
2132  
2133  
2134  
2135  
2136  
2137  
2138  
2139  
2140  
2141  
2142  
2143  
2144  
2145  
2146  
2147  
2148  
2149  
2150  
2151  
2152  
215

$$\frac{1}{R_{tot}(\text{pH})} = \sum \frac{1}{R^X(\text{pH})}. \quad (8)$$

The pH dependent resistance of either the neutral or ionized protonation species is available from:

$$R^X(\text{pH}) = \frac{1}{f^X(\text{pH})} \sum_{\text{layers}} \frac{dz}{K^X(z)D^X(z)}. \quad (9)$$

The particular fraction of the neutral or ionized species  $f^X(\text{pH})$  is calculated from the ionization fraction in the aqueous buffer solution surrounding the membrane system, which is related to the chemical specific  $\text{p}K_a$  values in aqueous systems. The individual dissociation constants of the possibly multiple protonation and deprotonation sites are calculated by *COSMOtherm*, derived from free energy differences between the particular species.<sup>38,39</sup> The population of the individual states follows from the partition function over all protonation states. The corresponding expressions are presented in section S2 of the supporting information.

The model assumes that the membrane potential does not change significantly, and that protonation or deprotonation reactions do not take place inside the membrane: acid-base reactions are very unlikely to occur in the alkyl tail part of the membrane, which imposes the main resistance of the permeation process for ions.

**Free Energy of Ions in the Membrane Center.** The probability for ions to be present in the non-polar center of a bilayer membrane is usually very low. This is in accordance with free energy profiles of ionic systems, which have their free energy minimum mostly close to the

1  
2  
3 phospholipids polar head group region.<sup>40</sup> However, the proper quantification of the free energy of  
4 ions in the membrane interior is mandatory for a mechanistic grasp of the penetration process.  
5  
6 Unfortunately, the classic COSMO-RS method has a known problem with respect to the exact  
7  
8 quantification of the free energy of ions in non-polar media, which usually is unimportant, given  
9  
10 that ions are anyway of negligible importance in such media. But, for the quantification of the  
11  
12 permeation of permanent ions through phospholipid membranes, it is necessary to use accurate  
13  
14 free energies. Fortunately, in non-polar solvents the dielectric continuum approach is well justified,  
15  
16 and the bare COSMO energies can be used in combination with a dielectric scaling factor. The  
17  
18 COSMO-RS dielectric energy ( $E_{\text{diel}}$ ) is defined as half of the electrostatic interaction energies of  
19  
20 the ideally screened polarized solutes ( $\epsilon_S = \infty$ ) with their screening charges,<sup>11</sup> which needs to be  
21  
22 corrected to the alkyl chain environment ( $\epsilon_{\text{alkyl}} = 2.1$ ):<sup>41</sup>  
23  
24  
25  
26  
27  
28  
29  
30

$$\Delta G_{\text{Born}}^{\text{ion}} = \left[ 1 - \left( \frac{\epsilon_{\text{alkyl}} - 1}{\epsilon_{\text{alkyl}}} \right) \right] E_{\text{diel}} \quad (10)$$

31  
32  
33  
34  
35  
36 The final free energy profile  $\Delta G(z)$  is then obtained by correcting the COSMOmic free energy  
37  
38  $\Delta G_{\text{mic}}(z)$  (**equation 5**) in the following way for ions:  
39  
40  
41  
42

$$\Delta G(z) = \Delta G_{\text{mic}}(z) + p_{\text{Born}}(z) [\Delta G_{\text{Born}}^{\text{ion}} - \mu_{\text{misfit}}^{\text{ion}}]_{\text{alkyl}} \quad (11)$$

43  
44  
45  
46  
47 Here,  $\mu_{\text{misfit}}$  is the original misfit contribution to the chemical potential of the ion at infinite dilution,  
48  
49 which is replaced by the Born energy in the alkyl chain environment. And  $p_{\text{Born}}(z)$  is a weight  
50  
51 factor for the correction term, approaching zero at the region of the polar head groups holding  
52  
53 significantly larger  $\epsilon$  values as compared to the alkane environment:  
54  
55  
56  
57  
58  
59  
60

$$p_{\text{Born}}(z) = \exp\left[-f_{\text{Born}}\left(\frac{\epsilon(z) - \epsilon_{\text{alkyl}}}{\epsilon_{\text{alkyl}}}\right)^2\right] \quad (12)$$

The factor of the Born correction  $f_{\text{Born}}$  is an empirical parameter (and fixed to a value of 3 throughout this manuscript from free energy considerations for typical ions, further details not shown). Thus, the factor is not dependent on the type of the permeating ion. This function is relatively steep, keeping in mind that this correction term shall just correct for the free energies of ions in the alkyl tails, whereas interactions between ions and more polar parts of the phospholipids are well predicted by COSMO-RS. All remaining parameters result consistently from mechanistic COSMO-RS calculations.

**Software.** The quantum chemical COSMO files are needed for all involved relevant conformers of all solutes and their corresponding ions (if applicable) in the penetration process. The software BIOVIA COSMO*conf* is used for full energy minimization and conformer generation, utilizing the quantum chemical TURBOMOLE software.<sup>42,43</sup> Membrane free energy profiles, diffusion coefficients,  $pK_a$  values in the water phase and layer-specific electrostatic parameters for the Born correction are calculated using the COSMO*perm* module of BIOVIA COSMO*therm* 2019.<sup>44</sup> The currently best performance is achieved with a full optimization of the molecular geometry using the def-TZVP basis set (in short: “TZVP” level) and subsequent COSMO single point calculations using the def2-TZVPD basis set with additional diffuse basis functions and a novel fine grid cavity (in short: “TZVPD-FINE” level).<sup>45</sup> All calculations are performed at both levels, TZVP and TZVPD-FINE. If not indicated otherwise, the presented values (incl. diagrams and tables) are calculated by the more accurate TZVPD-FINE level.

## RESULTS AND DISCUSSION

**Free Energy and Resistance Profile in Membrane Layers.** Free energy profiles and local resistances of the caproic acid as a typical example system are shown in **Figure 1a and 1b**, respectively. The local resistance opposing permeability is obtained by a combination of local diffusion coefficients and the height of the energy barrier (**equation 9**). The free energy profiles and, thus, the resistance profiles deviate significantly for the neutral species (blue lines) and the ionized species (red lines). It becomes obvious that there are two parts of the membrane, which are responsible for the main resistance in the permeation process. The first one is located at the central alkyl part of the membrane for both protonation states. Here the energy barrier is considerably higher for the ionized species.

Phospholipid membranes are considered as almost impermeable for ions (without the presence of membrane transporter proteins, which are not considered in this work), as it is certainly true for caproic acid. This assumption is probably also true for most pharmaceuticals; nevertheless, examples of ions permeating through phospholipid membranes to a significant extent by the passive, diffusion-controlled mechanism are discussed below. The central alkyl part is considered as the main barrier because polar organic chemicals will find this region rather unattractive. Many published approaches simplify the permeation process by a classic solubility-diffusion model through an alkane phase, e.g., hexadecane;<sup>3,27,31</sup> or even by using the octanol-water partition coefficient as classical descriptor.<sup>5</sup> The latter correlates strongly with the partitioning of neutral compounds into phospholipid membranes.<sup>46</sup> However, a second barrier shows up in our

1  
2  
3 calculations, which is located at the interface between the zwitterions in the polar head group and  
4 water. This barrier can be explained due to unfavorable interactions between the permeant and the  
5 zwitterionic polar head group. For the neutral state, a second free energy barrier does not show up.  
6  
7  
8 But there is a local maximum of the resistance profile (at  $z = 19 \text{ \AA}$ ), related to a reduction of the  
9  
10 diffusion coefficients at this point. The possibility of different rate-limiting barriers for different  
11  
12 kinds of solutes has also been considered by several investigators.<sup>7,47,48,49</sup> In more detail,  
13  
14 hydrophobic solutes may be rate-limited by diffusion through the peripheral region of the bilayer,  
15  
16 which is more polar and more structured.<sup>5</sup> Indeed, this might be confirmed by running calculations  
17  
18 for highly hydrophobic alkanes (see discussion in the supporting information, chapter S4). For  
19  
20 more hydrophilic solutes, this could be related to electrostatic interactions between the negatively  
21  
22 charged phosphate group of DMPC and solute anions (or negatively polarized surface areas of the  
23  
24 solute); or vice versa, between the positively charged cholin group of DMPC and solute cations  
25  
26 (or positively polarized surface areas of the solute). Especially in case of very high membrane  
27  
28 permeability, the second barrier may constitute the rate-limiting step; at this point, the mechanistic  
29  
30 COSMO<sub>perm</sub> model would outplay the classic approaches. A selection of predicted free energy  
31  
32 barriers is shown in **Figure 2** for aspirin, sulfasalazine and lincomycin, illustrating the potential  
33  
34 importance of this second barrier. This barrier might even be the rate-limiting step for  
35  
36 sulfasalazine.  
37  
38  
39  
40  
41  
42  
43  
44  
45  
46

47 For ionizable chemicals, the actual site of deprotonation and protonation reactions is still a matter  
48  
49 of debate. The prevalent ionic species might pass the aqueous boundary layer (ABL) and then  
50  
51 transform into the corresponding neutral species close to the membrane surface.<sup>26</sup> However, how  
52  
53 far these deprotonation and protonation reactions reach into the membrane itself is yet unclear.  
54  
55  
56  
57  
58  
59  
60

1  
2  
3 ABL-related effects will be investigated in further mechanistic studies related to the mechanistic  
4  
5 COSMO $perm$  model.  
6  
7  
8  
9

10 **Permeability of Neutral Compounds.** The correlation between experimental BLM  
11 permeabilities and predicted COSMO $perm$  permeabilities (using the DMPC system as reference)  
12 is shown in **Figure 3** (neutral: black symbols). The statistical analysis listed in **Table 2** shows  
13 squared correlation coefficients of  $r^2 = 0.91$  [0.81] and deviations of  $rmsd = 0.84$  [1.06]  $\log_{10}$  units  
14 to the experiment for neutral compounds at the TZVPD-FINE [TZVP] level. By correcting the  
15 values slightly for the linear regression slope and intercept, the deviations decrease to  $rmsd = 0.69$   
16 [0.98]. The value range ( $-7.96 \dots +1.70 \log_{10}$  units) covers ten orders of magnitude. Low  
17 molecular volume compounds with an atom count  $\leq 5$  (e.g., HF, HCl, HSCN, HNO<sub>3</sub>;) are not part  
18 of the statistics, related to partially deviating permeation mechanisms.<sup>3,16</sup>  
19  
20  
21  
22  
23  
24  
25  
26  
27  
28  
29

30 Overall, the more accurate TZVPD-FINE level is recommended for the predictive calculation of  
31 permeability values of neutral compounds. These results are in a similar range as derived from a  
32 published BLM model ( $r^2 = 0.91$ ;  $rmsd = 0.64$ ) utilizing – mostly experimentally determined –  
33 pp-LFER (poly-parameter Linear Free Energy Relationship) parameters.<sup>3</sup>  
34  
35  
36  
37  
38  
39

40 At a first glance, the slope deviates slightly from unity for the neutral dataset (1.3 and 1.2 at the  
41 TZVPD-FINE and TZVP level, respectively), which can be partially explained by the deviations  
42 to the experiment at the high permeability end. Here, the aqueous boundary layer (ABL) might be  
43 accounted for in a different way by the experiment and the calculations. The ABL is not considered  
44 as rate-limiting in most of the cases in our dataset, so the few surrounding pure water layers  
45 ( $\sim 5 \text{ \AA}$ ) are treated in the same way as layers containing phospholipids. Effects introduced by  
46 buffer components in the experiments might play an additional role, which are also not considered  
47  
48  
49  
50  
51  
52  
53  
54  
55  
56  
57  
58  
59  
60

1  
2  
3 by the model at the current stage. As will be shown below, the combined dataset of neutral  
4 compounds and anions – which covers a larger value range – leads to a slope and intercept close  
5  
6 to unity, so it might not be necessary to correct for the slope.  
7  
8  
9

10  
11  
12 **Permeability of Anions.** The advantage of the COSMO $_{perm}$  model is the simultaneous  
13 handling of neutral and ionic species, without any recalibrations of the underlying COSMO-RS or  
14 COSMO $_{mic}$  method. The correlation between BLM permeability values and predicted  
15 COSMO $_{perm}$  permeability values is shown in **Figure 3** (anions: blue symbols), and the  
16 corresponding statistics listed in **Table 2**. The value range ( $-11.5 \dots +2.2 \log_{10}$  units) covers  
17 fourteen orders of magnitude.  
18  
19

20  
21  
22 A squared correlation coefficient of  $r^2 = 0.94$  [0.89] and a deviation of  $rmsd = 1.00$  [1.40]  $\log_{10}$   
23 units is obtained for ions at the TZVPD-FINE [TZVP] level. Slight corrections for slope and  
24 intercept improve the  $rmsd$  values to 0.93 [1.26]. Not part of the statistics are ions with only an  
25 upper threshold as the experimental information, but without knowledge of the exact value. The  
26 Born correction (**equation 11**) is applied in all TZVP calculations, which is already implicit part  
27 of the TZVPD-FINE parameterization (details not shown).  
28  
29

30  
31  
32 At the TZVPD-FINE level, predictions for compounds prone to strong push-pull effects are  
33 corrected by a constant offset of  $-2.5$ , as indicated in **Table 1**. These strong push-pull effects are  
34 characterized by strong deactivating groups (i.e.,  $-\text{NO}_2$ ,  $-\text{C}\equiv\text{N}$ ,  $-\text{CO}_2\text{R}$ ; with both  $-\text{I}$  inductive  
35 and  $-\text{M}$  resonance effects) *directly conjugated* to extremely activating groups (i.e.,  $-\text{O}^-$  anion).  
36  
37 This is not a limitation of the COSMO $_{perm}$  method or COSMO-RS theory as such, but of the  
38 underlying quantum chemical calculation method, i.e. density functional theory, which tends to  
39 overestimate charge separation effects.<sup>50</sup> The TZVP results apparently are less sensitive to this  
40  
41  
42  
43  
44  
45  
46  
47  
48  
49  
50  
51  
52  
53  
54  
55  
56  
57  
58  
59  
60

1  
2  
3 overestimation and the application of this correction term turned out to be needless due to fortunate  
4  
5 error cancellation.  
6

7  
8 The statistics of the TZVP level is significantly better when removing the largest outlier DPA  
9  
10 (2,4,6-trinitro-N-(2,4,6-trinitrophenyl)aniline, pred.  $-3.32$ , exp.  $0.90$ ). In this case, the correlation  
11  
12 coefficient of the dataset improves to  $r^2 = 0.93$  with a deviation of  $rmsd = 0.93 \log_{10}$  units. Note  
13  
14 that this compound is no outlier at the TZVPD-FINE level, which demonstrates a better handling  
15  
16 of anilines by the latter.  
17

18  
19 In general, both the TZVPD-FINE and the TZVP level could be used for calculating permeability  
20  
21 values of anions. By combining the datasets of neutral compounds and anions at the TZVPD-FINE  
22  
23 level, slopes close to one ( $0.99$ ) and intercepts close to zero ( $-0.06$ ) are obtained, illustrating the  
24  
25 predictive character of *COSMOperm* without the requirement for a system-specific calibration,  
26  
27 while it must be admitted that the almost exact slope of  $0.99$  might be a lucky coincidence. The  
28  
29 TZVP level turned out to be slightly more predictive, as it did not require the push-pull-effect  
30  
31 correction.  
32  
33

34  
35 A slight non-linearity might occur in the close inspection of **Figure 3** at the low and high  
36  
37 permeability ends. This might be related to both the predictions as well as difficulties in the  
38  
39 measurements at boundaries of the permeability scale. Because the exact reason is not known, we  
40  
41 refrained to apply a polynomial fit; nevertheless, it could be used to improve the statistics as part  
42  
43 in further model refinements.  
44  
45

46  
47 To the best of our knowledge, this is the first mechanistic membrane permeability model, on the  
48  
49 one hand operating at the atomistic level of phospholipid membranes, and on the other hand  
50  
51 leading to an accuracy of better than one logarithmic unit for both neutral compounds and ions.  
52  
53 Even more, the calculation times are in the range of a few minutes, with the potential to apply  
54  
55  
56  
57  
58  
59  
60

1  
2  
3 COSMO $Perm$  in both screening applications and detailed investigations of membrane  
4 permeabilities.  
5  
6  
7  
8  
9

10 **Permeability of Cations.** There is a sparse availability of data for the permeability of  
11 cations, because cations traverse the membrane orders of magnitude slower than structurally  
12 similar anions due to the positive membrane dipole potential.<sup>35</sup> The few available permeation data  
13 differ widely between different assays, as for cations various membrane types are used that often  
14 show an increased membrane permeability, to compensate for the decrease in the electrical signal  
15 of experimental measurements. Herein, the membrane systems for cations are composed of: (a)  
16 asolectin; (b) pure 1,2-di-O-phytanyl-*sn*-glycero-3-phosphocholine (DPhytanylPC), or (c) with  
17 additional 5  $\mu$ M phloretin; and (d) 1,2-diphytanoyl-*sn*-glycero-3-phosphocholine or 1,2-dioleoyl-  
18 *sn*-glycero-3-phosphocholine (DPhPC/DOPC). The increase of the membrane permeability is  
19 probably related to the decrease of the membrane dipole potential. For example, DPhytanylPC  
20 contains ether linkages, and the absence of carbonyl groups causes a decrease in the dipole  
21 potential of more than 100 mV as compared to membranes formed from lipids containing ester  
22 linkages.<sup>51,52</sup> Our analysis of COSMO $Perm$  performance in predicting cationic permeability data  
23 is in consequence mainly based on the systematic measurements of cationic permeability of  
24 tetraphenylphosphonium and six of its analogues<sup>53</sup>, and of *n*-dodecyltriphenylphosphonium and  
25 seven of its analogues<sup>51</sup>.  
26  
27  
28  
29  
30  
31  
32  
33  
34  
35  
36  
37  
38  
39  
40  
41  
42  
43  
44  
45

46 In an initial analysis, all cation-specific membrane types (except DPhPC/DOPC) are used in a  
47 common dataset compilation and correlated to COSMO $Perm$  predictions with the full DMPC  
48 membrane (see **Figure 4a**). The slope turns out to be close to one (0.95), but the correlation  
49  
50  
51  
52  
53  
54  
55  
56  
57  
58  
59  
60

1  
2  
3 coefficient rather moderate ( $r^2 = 0.77$ ), especially related to cations at the high permeability end.  
4  
5 Nevertheless, the agreement to the asolectin assay could be interpreted as rather good ( $r^2 = 0.91$ ).  
6  
7  
8  
9

10 In a second attempt, the membrane layers between the two proposed resistance wells, i.e., two  
11 times the innermost 12 layers are used to calculate the membrane permeability ( $P = \frac{1}{2\sum_{i=1}^{12} R_i}$ ). The  
12  
13 reason is to avoid the influence of headgroups potentially overruling the membrane core (see  
14  
15 **Figure S4.2**). Indeed, the qualitative differences in membrane core resistance are captured quite  
16  
17 well between compounds in correlation to experimental permeability (see **Figure 4b**). Thus,  
18  
19 COSMO $perm$  seems to underestimate the cation resistance in the membrane core systematically,  
20  
21 and to rather overestimate the resistance in the headgroups. There are several reasons, which might  
22  
23 explain this effect:  
24  
25  
26  
27  
28

29 (1) The membrane dipole potential has been fitted to reproduce membrane/water partition  
30 coefficients ( $\log K_{m,w}$ ). The shape of this potential might be less sensitive to both the prediction of  
31  
32  $\log K_{m,w}$  values and the prediction of anion permeabilities than to the prediction of cation  
33  
34 permeabilities. Note that the dipole potential is used in an entirely predictive manner for  
35  
36 COSMO $perm$  and has not been refitted herein. See section S3 in the supporting information for  
37  
38 further details.  
39  
40  
41  
42

43 (2) The calculated conformer set contains mainly stretched conformers for these large  
44  
45 dodecylphosphonium derivatives. This is not relevant in classic COSMO-RS bulk phase  
46  
47 calculations; therefore a large portion of tilted conformers is typically dropped by the COSMO $conf$   
48  
49 conformer generation algorithm applied, unless they had an effect on the chemical potential.  
50  
51 However, tilted conformers might contribute significantly to the properties of inhomogenous  
52  
53 systems.<sup>21</sup>  
54  
55  
56  
57  
58  
59  
60

1  
2  
3 (3) The dodecylphosphonium derivatives have a similar extension as the membrane itself,  
4 potentially hitting the limitation of the infinite-dilution limit of the classic COSMOmic approach.

5  
6 Also, their sizes might be limiting the calculation, because they could potentially disturb the  
7 membrane structure. This could be overcome by a combined application of COSMOplex and  
8 COSMOperm to reach finite concentration effects, which is beyond the scope of this manuscript.

9  
10  
11 (4) The free energy profiles are probably influenced by salt or buffer concentrations in the aqueous  
12 phase, including potential protonation or deprotonation reactions close to the zwitterionic  
13 headgroups, which are not considered at the current stage.

14  
15 While Rokitskaya *et al.* did not observe a correlation between hydrophobicity and membrane  
16 permeability, lower COSMOperm resistances in the membrane core are directly related to higher  
17 experimental membrane permeabilities, and thus suggest a correlation between membrane  
18 permeability and compound hydrophobicity. The only exception to this rule are the three most  
19 hydrophobic dodecyltriphenylphosphonium derivatives (tri(3,5-dimethylphenyl), tri(2,4,6-  
20 trimethylphenyl), trinaphthyl). The measured permeabilities are underestimated, possibly because  
21 membrane permeability may already have reached a decreasing range at the measured  
22 concentration of 0.1–1.8  $\mu\text{M}$ ; and saturation effects seem to set in at lower compound  
23 concentration the higher the membrane permeability of a compound.<sup>31</sup> The three values were thus  
24 not considered in the following fit.

25  
26  
27 To address the systematic overestimation of membrane permeability, we fitted a linear correlation  
28 to each group of data points from literature measured in the different membrane types mentioned  
29 above. We assumed a systematic shift between different lipid groups, most likely due to a change  
30 in membrane dipole potential, and thus applied a membrane specific shift along with a global fit  
31 of the slope that is in best agreement with data points for all four assays (a-d). For the  
32  
33  
34  
35  
36  
37  
38  
39  
40  
41  
42  
43  
44  
45  
46  
47  
48  
49  
50  
51  
52  
53  
54  
55  
56  
57  
58  
59  
60

1  
2  
3 DPhPC/DOPC membranes, only permeability data for two different compounds were available,  
4  
5 therefore the correlation for this membrane system, which should resemble that of our DMPC  
6  
7 predictions most, is fit by using the fixed slope extracted from the other three curves. These  
8  
9 correlations, stated in **Figure 4b**, may be used to predict cationic membrane permeability for a  
10  
11 respective membrane type.  
12  
13  
14  
15  
16

17 **pH Dependence of Permeability.** The pH dependence of the predicted salicylic acid  
18  
19 permeability is compared to BLM values in the literature.<sup>27</sup> The pH dependence of individual  
20  
21 protonation states, predicted by *COSMOperm*, is then calculated by using the predicted BLM  
22  
23 values in **equation 9**, and eventually the total pH dependent BLM permeability of all protonation  
24  
25 states by **equation 8**. The good agreement of the *COSMOperm* model with the experiment is  
26  
27 shown in **Figure 5**. Slope and intercept are almost one and zero, respectively, and the *rmsd* value  
28  
29 as low as 0.08 log<sub>10</sub> units.  
30  
31  
32

33 Note that the experimental values refer to the intrinsic membrane permeability; the unstirred water  
34  
35 layer has been deducted from these values. An accurate description of the unstirred water layer is  
36  
37 potentially adjuvant for many permeability assays (e.g., BLM, Caco-2, PAMPA and several  
38  
39 more);<sup>3</sup> however, this is beyond the scope of this manuscript focusing on the intrinsic membrane  
40  
41 permeability alone. This topic will be further investigated in upcoming publications.  
42  
43  
44  
45  
46

47 **Permeability in Different Membrane Systems.** All results presented up to now are  
48  
49 validated against classic phospholipid membranes, mostly stabilized by viscous, non-polar alkane  
50  
51 solvents in the experiments. One strength of the *COSMOperm* method is its applicability to  
52  
53 membrane systems in general, as long as two conditions are met: First, an atomistic membrane  
54  
55  
56  
57  
58  
59  
60

1  
2  
3 structure can be generated, and second, the membrane system is at the liquid-crystalline state (for  
4 the validity of the fluid phase COSMO-RS equations).<sup>12</sup>  
5  
6

7 To illustrate this general applicability, a DMPC and chlorodecane containing membrane at the  
8 interface to water has been generated using COSMOplex. The experimental validation dataset is  
9 extracted from the supporting information of Ebert *et al.*<sup>31</sup> and shown in **Table 3**. The predicted  
10 COSMOperm values of the chlorodecane containing system are compared to the predicted values  
11 of the pure DMPC system (additional experimental and predicted values for the  
12 chlorodecane/decane/phospholipid system are listed in **Table S5.1** of the supporting information).  
13 On average, the permeability values are two to three orders of magnitude higher in the  
14 chlorodecane containing system (mean: -3.33; median: -3.04), a consequence of the increase of  
15 the dielectric constant inside the membrane core due to the chlorodecane.  
16  
17  
18  
19  
20  
21  
22  
23  
24  
25  
26  
27

28 A similar decrease of the membrane barrier for chlorodecane containing BLM by about three  
29 orders of magnitude is reported several times in the literature.<sup>31,54</sup> Chlorodecane containing  
30 membranes are used as a reference system for mitochondrial membranes, as their anionic  
31 permeability was shown to be very similar.<sup>54,55</sup> The reason for this similarity is believed to lie in  
32 the high amount of proteins present in the mitochondrial membrane, which supposedly causes a  
33 similar change in dielectric constant as chlorodecane.<sup>54</sup>  
34  
35  
36  
37  
38  
39  
40  
41

42 Further investigations will include more complex cell plasma membrane structures, which are  
43 formed by a complex mixture of phosphatidylcholines, -serines, and -ethanolamines,  
44 sphingomyelin, glycolipids and especially a varying amount of cholesterol.<sup>56</sup> These membrane  
45 structures could be generated using the COSMOplex method<sup>57</sup> and the corresponding solute  
46 permeabilities predicted by COSMOperm.  
47  
48  
49  
50  
51  
52  
53  
54  
55  
56  
57  
58  
59  
60

## CONCLUSIONS

Because of its generality, good predictivity and sound mechanistic treatment, the *COSMOperm* approach is a valuable tool for predicting the membrane permeability for a wide variety of neutral and ionic organic compounds. In addition, the  $\Delta G(z)$  and  $D(z)$  profiles are obtained quickly as a matter of a few minutes, as compared to time-consuming molecular dynamics simulations. This model allows for the examination of pH dependent effects on the passive permeation through phospholipid membranes, where these effects are captured on an atomic scale in a fully mechanistic way. The *COSMOperm* approach can be generally applied to any kind of membranes without the need for a re-calibration, as demonstrated by the artificial chlorodecane containing phospholipid system (generated by the *COSMOplex* method), or further possibilities, including cholesterol containing systems or skin lipid systems (e.g., in the *stratum corneum*).<sup>57</sup> Additional investigations include the integration of the *COSMOperm* approach into more complex systems involving aqueous boundary layers or living cell systems (e.g., Caco-2). The currently present infinite dilution approximation of *COSMOperm* can be overcome by a combination of the *COSMOperm* and *COSMOplex* approaches. The latter has extended the original *COSMOmic* applicability domain to finite concentration ranges. *COSMOperm* is designed and works well for membranes at the liquid-crystalline state. Further investigations are required, and additional terms need to be implemented for a proper description at the gel-phase state below the phase transition temperature.

1  
2  
3  
4  
5  
6 ASSOCIATED CONTENT  
7

8 **Supporting Information.** The supporting information contains details of the diffusion coefficient  
9 model, calculation of fractions of individual protonation states, details on the membrane models,  
10 and additional cation and chlorodecane containing membrane data. This material is available free  
11 of charge via the Internet at <http://pubs.acs.org>.  
12  
13

14  
15  
16 AUTHOR INFORMATION  
17

18 **Corresponding Author**  
19

20 \* Johannes Schwöbel, BIOVIA Dassault Systèmes Deutschland GmbH, Imbacher Weg 46, 51379  
21  
22 Leverkusen, Germany. E-mail: [Johannes.SCHWOEBEL@3ds.com](mailto:Johannes.SCHWOEBEL@3ds.com). Tel.: +49 2171 363664.  
23  
24

25  
26  
27 **Author Contributions**  
28

29 The manuscript was written through contributions of all authors. All authors have given approval  
30 to the final version of the manuscript.  
31  
32  
33

34  
35  
36 **Notes**  
37

38 The authors declare the following competing financial interest(s): Andreas Klamt, Johannes  
39 Schwöbel and Uwe Huniar are employees of Dassault Systèmes. Dassault Systèmes commercially  
40 distributes the BIOVIA *COSMOtherm*, BIOVIA *COSMOconf* and TURBOMOLE software  
41 packages used in this paper, including the *COSMOperm* and *COSMOplex* extensions.  
42  
43  
44  
45  
46  
47  
48  
49

50 **ACKNOWLEDGMENT**  
51

52  
53 This research was funded by the German Federal Ministry for Economic Affairs and Energy (ZIM,  
54  
55 Zentrales Innovationsprogramm Mittelstand, COSMOperm Project KF 3385901SB4).  
56  
57  
58  
59  
60

## REFERENCES

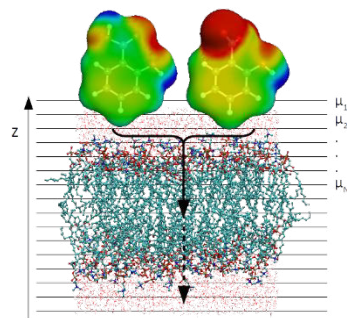
- (1) Lopes, D.; Jakobtorweihen, S.; Nunes, C.; Sarmiento, B.; Reis, S. Shedding Light on the Puzzle of Drug-Membrane Interactions: Experimental Techniques and Molecular Dynamics Simulations. *Prog. Lipid Res.* **2017**, *65*, 24–44.
- (2) Hanneschlaeger, C.; Horner, A.; Pohl, P. Intrinsic Membrane Permeability to Small Molecules. *Chem. Rev.* **2019**, *119* (9), 5922–5953.
- (3) Bittermann, K.; Goss, K.-U. Predicting Apparent Passive Permeability of Caco-2 and MDCK Cell-Monolayers: A Mechanistic Model. *PLOS ONE* **2017**, *12* (12), e0190319.
- (4) Nitsche, J. M.; Kasting, G. B. A Correlation for 1,9-Decadiene/Water Partition Coefficients. *J. Pharm. Sci.* **2013**, *102* (1), 136–144.
- (5) Walter, A.; Gutknecht, J. Permeability of Small Nonelectrolytes through Lipid Bilayer Membranes. *J. Membr. Biol.* **1986**, *90* (3), 207–217.
- (6) Parisio, G.; Stocchero, M.; Ferrarini, A. Passive Membrane Permeability: Beyond the Standard Solubility-Diffusion Model. *J. Chem. Theory Comput.* **2013**, *9* (12), 5236–5246.
- (7) Diamond, J. M.; Katz, Y. Interpretation of Nonelectrolyte Partition Coefficients between Dimyristoyl Lecithin and Water. *J. Membr. Biol.* **1974**, *17* (1), 121–154.
- (8) Bennion, B. J.; Be, N. A.; McNerney, M. W.; Lao, V.; Carlson, E. M.; Valdez, C. A.; Malfatti, M. A.; Enright, H. A.; Nguyen, T. H.; Lightstone, F. C.; et al. Predicting a Drug's Membrane Permeability: A Computational Model Validated with in Vitro Permeability Assay Data. *J. Phys. Chem. B* **2017**, *121* (20), 5228–5237.
- (9) Menichetti, R.; Kanekal, K. H.; Bereau, T. Drug-Membrane Permeability across Chemical Space. *ACS Cent. Sci.* **2019**, *5* (2), 290–298.
- (10) Klamt, A.; Eckert, F. COSMO-RS: A Novel and Efficient Method for the a Priori Prediction of Thermophysical Data of Liquids. *Fluid Phase Equilib.* **2000**, *172* (1), 43–72.
- (11) Klamt, A.; Jonas, V.; Bürger, T.; Lohrenz, J. C. Refinement and Parametrization of COSMO-RS. *J. Phys. Chem. A* **1998**, *102* (26), 5074–5085.
- (12) Klamt, A.; Huniar, U.; Spycher, S.; Keldenich, J. COSMOmic: A Mechanistic Approach to the Calculation of Membrane-Water Partition Coefficients and Internal Distributions within Membranes and Micelles. *J. Phys. Chem. B* **2008**, *112* (38), 12148–12157.
- (13) Paloncýová, M.; DeVane, R.; Murch, B.; Berka, K.; Otyepka, M. Amphiphilic Drug-like Molecules Accumulate in a Membrane below the Head Group Region. *J. Phys. Chem. B* **2014**, *118* (4), 1030–1039.
- (14) Ritter, E.; Yordanova, D.; Gerlach, T.; Smirnova, I.; Jakobtorweihen, S. Molecular Dynamics Simulations of Various Micelles to Predict Micelle Water Partition Equilibria with COSMOmic: Influence of Micelle Size and Structure. *Fluid Phase Equilib.* **2016**, *422*, 43–55.
- (15) Jakobtorweihen, S.; Zuniga, A. C.; Ingram, T.; Gerlach, T.; Keil, F. J.; Smirnova, I. Predicting Solute Partitioning in Lipid Bilayers: Free Energies and Partition Coefficients from Molecular Dynamics Simulations and COSMOmic. *J. Chem. Phys.* **2014**, *141* (4), 045102.
- (16) Lomize, A. L.; Pogozheva, I. D. Physics-Based Method for Modeling Passive Membrane Permeability and Translocation Pathways of Bioactive Molecules. *J. Chem. Inf. Model* **2019**, *59* (7), 3198–3213.

- 1
- 2
- 3
- 4 (17) McLaughlin, S. The Mechanism of Action of DNP on Phospholipid Bilayer Membranes. *J. Membrane Biol.* **1972**, *9* (1), 361–372.
- 5
- 6 (18) Stark, G.; Ketterer, B.; Benz, R.; Läuger, P. The Rate Constants of Valinomycin-Mediated Ion Transport through Thin Lipid Membranes. *Biophys. J.* **1971**, *11* (12), 981–994.
- 7
- 8 (19) Pohl, E. E.; Krylov, A. V.; Block, M.; Pohl, P. Changes of the Membrane Potential Profile Induced by Verapamil and Propranolol. *Biochim. Biophys. Acta Biomembr.* **1998**, *1373* (1), 170–178.
- 9
- 10
- 11 (20) Hanneschlaeger, C.; Pohl, P. Membrane Permeabilities of Ascorbic Acid and Ascorbate. *Biomolecules* **2018**, *8* (3), 73.
- 12
- 13 (21) Klamt, A.; Schwöbel, J.; Huniar, U.; Koch, L.; Terzi, S.; Gaudin, T. COSMOplex: Self-Consistent Simulation of Self-Organizing Inhomogeneous Systems Based on COSMO-RS. *Phys. Chem. Chem. Phys.* **2019**, *21* (18), 9225–9238.
- 14
- 15 (22) Bittermann, K.; Spycher, S.; Endo, S.; Pohler, L.; Huniar, U.; Goss, K.-U.; Klamt, A. Prediction of Phospholipid-Water Partition Coefficients of Ionic Organic Chemicals Using the Mechanistic Model COSMOmic. *J. Phys. Chem. B* **2014**, *118* (51), 14833–14842.
- 16
- 17 (23) Bittermann, K.; Spycher, S.; Goss, K.-U. Comparison of Different Models Predicting the Phospholipid-Membrane Water Partition Coefficients of Charged Compounds. *Chemosphere* **2016**, *144*, 382–391.
- 18
- 19 (24) Mueller, P.; Rudin, D. O.; Ti Tien, H.; Wescott, W. C. Reconstitution of Cell Membrane Structure in Vitro and Its Transformation into an Excitable System. *Nature* **1962**, *194* (4832), 979–980.
- 20
- 21 (25) Montal, M.; Mueller, P. Formation of Bimolecular Membranes from Lipid Monolayers and a Study of Their Electrical Properties. *Proc. Natl. Acad. Sci. USA* **1972**, *69* (12), 3561–3566.
- 22
- 23 (26) Antonenko, Y. N.; Denisov, G. A.; Pohl, P. Weak Acid Transport across Bilayer Lipid Membrane in the Presence of Buffers. Theoretical and Experimental PH Profiles in the Unstirred Layers. *Biophys. J.* **1993**, *64* (6), 1701–1710.
- 24
- 25 (27) Gutknecht, J.; Tosteson, D. C. Diffusion of Weak Acids across Lipid Bilayer Membranes: Effects of Chemical Reactions in the Unstirred Layers. *Science* **1973**, *182* (4118), 1258–1261.
- 26
- 27 (28) Gutknecht, J.; Walter, A. Histamine, Theophylline and Tryptamine Transport through Lipid Bilayer Membranes. *Biochim. Biophys. Acta Biomembr.* **1981**, *649* (2), 149–154.
- 28
- 29 (29) Xiang, T. X.; Chen, X.; Anderson, B. D. Transport Methods for Probing the Barrier Domain of Lipid Bilayer Membranes. *Biophys. J.* **1992**, *63* (1), 78–88.
- 30
- 31 (30) Pohl, P.; Rokitskaya, T. I.; Pohl, E. E.; Saparov, S. M. Permeation of Phloretin across Bilayer Lipid Membranes Monitored by Dipole Potential and Microelectrode Measurements. *Biochim. Biophys. Acta Biomembr.* **1997**, *1323* (2), 163–172.
- 32
- 33 (31) Ebert, A.; Hanneschlaeger, C.; Goss, K.-U.; Pohl, P. Passive Permeability of Planar Lipid Bilayers to Organic Anions. *Biophys. J.* **2018**, *115* (10), 1931–1941.
- 34
- 35 (32) Klamt, A.; Schüürmann, G. COSMO: A New Approach to Dielectric Screening in Solvents with Explicit Expressions for the Screening Energy and Its Gradient. *J. Chem. Soc. Perkin 2* **1993**, *1993* (5), 799–805.
- 36
- 37 (33) Klamt, A. *COSMO-RS From Quantum Chemistry to Fluid Phase Thermodynamics and Drug Design*; Elsevier: Amsterdam, The Netherlands; Boston, MA, USA, 2005.
- 38
- 39 (34) Jakobtorweihen, S.; Ingram, T.; Smirnova, I. Combination of COSMOmic and Molecular Dynamics Simulations for the Calculation of Membrane-Water Partition Coefficients. *J. Comput. Chem.* **2013**, *34* (15), 1332–1340.
- 40
- 41
- 42
- 43
- 44
- 45
- 46
- 47
- 48
- 49
- 50
- 51
- 52
- 53
- 54
- 55
- 56
- 57
- 58
- 59
- 60

- 1  
2  
3 (35) Flewelling, R. F.; Hubbell, W. L. The Membrane Dipole Potential in a Total Membrane  
4 Potential Model. Applications to Hydrophobic Ion Interactions with Membranes. *Biophys. J.*  
5 **1986**, *49* (2), 541–552.
- 6 (36) Benz, R.; McLaughlin, S. The Molecular Mechanism of Action of the Proton Ionophore  
7 FCCP (Carbonylcyanide p-Trifluoromethoxyphenylhydrazone). *Biophys. J.* **1983**, *41* (3),  
8 381–398.
- 9 (37) Poling, B. E.; Prausnitz, J. M.; John Paul, O.; Reid, R. C. *The Properties of Gases and*  
10 *Liquids*; McGraw-Hill: New York, USA, 2001; Vol. 5.
- 11 (38) Klamt, A.; Eckert, F.; Diedenhofen, M.; Beck, M. E. First Principles Calculations of Aqueous  
12 PKa Values for Organic and Inorganic Acids Using COSMO-RS Reveal an Inconsistency in  
13 the Slope of the PKa Scale. *J. Phys. Chem. A* **2003**, *107* (44), 9380–9386.
- 14 (39) Eckert, F.; Diedenhofen, M.; Klamt, A. Towards a First Principles Prediction of pKa:  
15 COSMO-RS and the Cluster-Continuum Approach. *Molec. Phys.* **2010**, *108* (3–4), 229–241.
- 16 (40) Spycher, S.; Smejtek, P.; Netzeva, T. I.; Escher, B. I. Toward a Class-Independent  
17 Quantitative Structure-Activity Relationship Model for Uncouplers of Oxidative  
18 Phosphorylation. *Chem. Res. Toxicol.* **2008**, *21* (4), 911–927.
- 19 (41) Klamt, A.; Moya, C.; Palomar, J. A Comprehensive Comparison of the IEFPCM and  
20 SS(V)PE Continuum Solvation Methods with the COSMO Approach. *J. Chem. Theory*  
21 *Comput.* **2015**, *11* (9), 4220–4225.
- 22 (42) *COSMOconf 4.3*; BIOVIA Dassault Systèmes; <http://www.3ds.com>: Leverkusen, Germany,  
23 2018.
- 24 (43) *TURBOMOLE V7.3*; University of Karlsruhe and Forschungszentrum Karlsruhe GmbH,  
25 1989-2007, TURBOMOLE GmbH, since 2007; available from <http://www.turbomole.com>:  
26 Karlsruhe, Germany, 2018.
- 27 (44) *COSMOtherm, Release 19*; BIOVIA Dassault Systèmes; <http://www.3ds.com>: Leverkusen,  
28 Germany, 2019.
- 29 (45) Klamt, A.; Diedenhofen, M. A Refined Cavity Construction Algorithm for the Conductor-  
30 like Screening Model. *J. Comput. Chem.* **2018**, *39* (21), 1648–1655.
- 31 (46) Endo, S.; Escher, B. I.; Goss, K.-U. Capacities of Membrane Lipids to Accumulate Neutral  
32 Organic Chemicals. *Environ. Sci. Technol.* **2011**, *45* (14), 5912–5921.
- 33 (47) Zocher, F.; van der Spoel, D.; Pohl, P.; Hub, J. S. Local Partition Coefficients Govern Solute  
34 Permeability of Cholesterol-Containing Membranes. *Biophys. J.* **2013**, *105* (12), 2760–2770.
- 35 (48) Andersen, O. S. Permeability Properties of Unmodified Lipid Bilayer Membranes. In  
36 *Concepts and Models*; Tosteson, D. C., Ed.; Springer Berlin Heidelberg: Berlin, Heidelberg,  
37 1978; pp 369–446.
- 38 (49) Stein, W. D. Permeability for Lipophilic Molecules. In *New Comprehensive Biochemistry*;  
39 Elsevier, 1981; Vol. 2, pp 1–28.
- 40 (50) Reinisch, J.; Diedenhofen, M.; Wilcken, R.; Udvarhelyi, A.; Glöß, A. Benchmarking  
41 Different QM Levels for Usage with COSMO-RS. *J. Chem. Inf. Model.* **2019**, *59* (11), 4806–  
42 4813.
- 43 (51) Rokitskaya, T. I.; Luzhkov, V. B.; Korshunova, G. A.; Tashlitsky, V. N.; Antonenko, Y. N.  
44 Effect of Methyl and Halogen Substituents on the Transmembrane Movement of Lipophilic  
45 Ions. *Phys. Chem. Chem. Phys.* **2019**, *21* (42), 23355–23363.
- 46 (52) Shen, H.; Zhao, K.; Wu, Z. Effects of Ether Linkage on Membrane Dipole Potential and  
47 Cholesterol Flip-Flop Motion in Lipid Bilayer Membranes. *J. Phys. Chem. B* **2019**, *123* (37),  
48 7818–7828.
- 49  
50  
51  
52  
53  
54  
55  
56  
57  
58  
59  
60

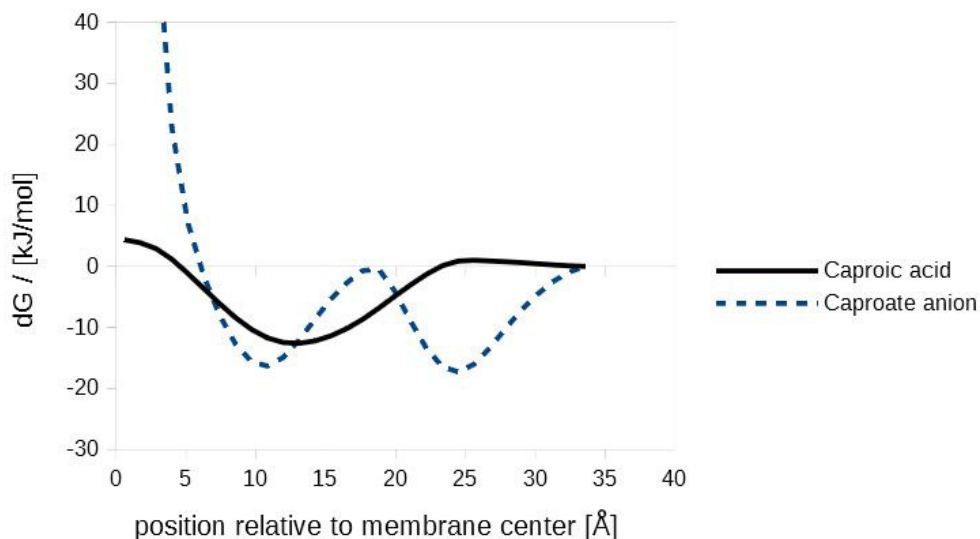
- 1  
2  
3 (53) Miyauchi, S.; Ono, A.; Yoshimoto, M.; Kamo, N. Membrane Transport of  
4 Tetrphenylphosphonium and Its Homologues through the Planar Phospholipid Bilayer:  
5 Concentration Dependence and Mutually Competitive Inhibition in Membrane Passive  
6 Transport. *J. Pharm. Sci.* **1993**, *82* (1), 27–31.
- 7  
8 (54) Dilger, J. P.; McLaughlin, S. G.; McIntosh, T. J.; Simon, S. A. The Dielectric Constant of  
9 Phospholipid Bilayers and the Permeability of Membranes to Ions. *Science* **1979**, *206* (4423),  
10 1196–1198.
- 11 (55) Gutknecht, J. Salicylates and Proton Transport through Lipid Bilayer Membranes: A Model  
12 for Salicylate-Induced Uncoupling and Swelling in Mitochondria. *J. Membr. Biol.* **1990**, *115*  
13 (3), 253–260.
- 14 (56) Alberts, B.; Johnson, A. D.; Lewis, J.; Morgan, D.; Raff, M.; Roberts, K.; Walter, P.  
15 *Molecular Biology of the Cell*, Sixth edition.; W. W. Norton & Company: New York, NY,  
16 2014.
- 17 (57) Schwöbel, J. A. H.; Klamt, A. Mechanistic Skin Penetration Model by the COSMOperm  
18 Method: Routes of Permeation, Vehicle Effects and Skin Variations in the Healthy and  
19 Compromised Skin. *Comput. Toxicol.* **2019**, *11*, 50–64.
- 20 (58) Gutknecht, J. Aspirin, Acetaminophen and Proton Transport through Phospholipid Bilayers  
21 and Mitochondrial Membranes. *Mol. Cell Biochem.* **1992**, *114* (1), 3–8.
- 22 (59) Finkelstein, A. Water and Nonelectrolyte Permeability of Lipid Bilayer Membranes. *J. Gen.*  
23 *Physiol.* **1976**, *68* (2), 127–135.
- 24 (60) Walter, A.; Gutknecht, J. Monocarboxylic Acid Permeation through Lipid Bilayer  
25 Membranes. *J. Membr. Biol.* **1984**, *77* (3), 255–264.
- 26 (61) Borisova, M. P.; Ermishkin, L. N.; Liberman, E. A.; Silberstein, A. Y.; Trofimov, E. M.  
27 Mechanism of Conductivity of Bimolecular Lipid Membranes in the Presence of  
28 Tetrachlorotrifluoromethylbenzimidazole. *J. Membr. Biol.* **1974**, *18* (1), 243–261.
- 29 (62) Kasianowicz, J.; Benz, R.; McLaughlin, S. The Kinetic Mechanism by Which CCCP  
30 (Carbonyl Cyanidem-Chlorophenylhydrazone) Transports Protons across Membranes. *J.*  
31 *Membr. Biol.* **1984**, *82* (2), 179–190.
- 32 (63) Cohen, F. S.; Eisenberg, M.; McLaughlin, S. The Kinetic Mechanism of Action of an  
33 Uncoupler of Oxidative Phosphorylation. *J. Membr. Biol.* **1977**, *37* (1), 361–396.
- 34 (64) Pickar, A. D.; Benz, R. Transport of Oppositely Charged Lipophilic Probe Ions in Lipid  
35 Bilayer Membranes Having Various Structures. *J. Membr. Biol.* **1978**, *44* (3–4), 353–376.
- 36 (65) McLaughlin, S.; Eisenberg, M.; Cohen, F.; Dilger, J. The Unique Ability of Picrate to  
37 Uncouple Submitochondrial Particles but Not Mitochondria Is Consistent with the  
38 Chemiosmotic Hypothesis. In *Frontiers of Biological Energetics*; Dutton, P. L., Leigh, J. S.,  
39 Scarpa, A., Eds.; 1978; Vol. 2, pp 1205–1213.
- 40  
41  
42  
43  
44  
45  
46  
47  
48  
49  
50  
51  
52  
53  
54  
55  
56  
57  
58  
59  
60

TOC Graphics

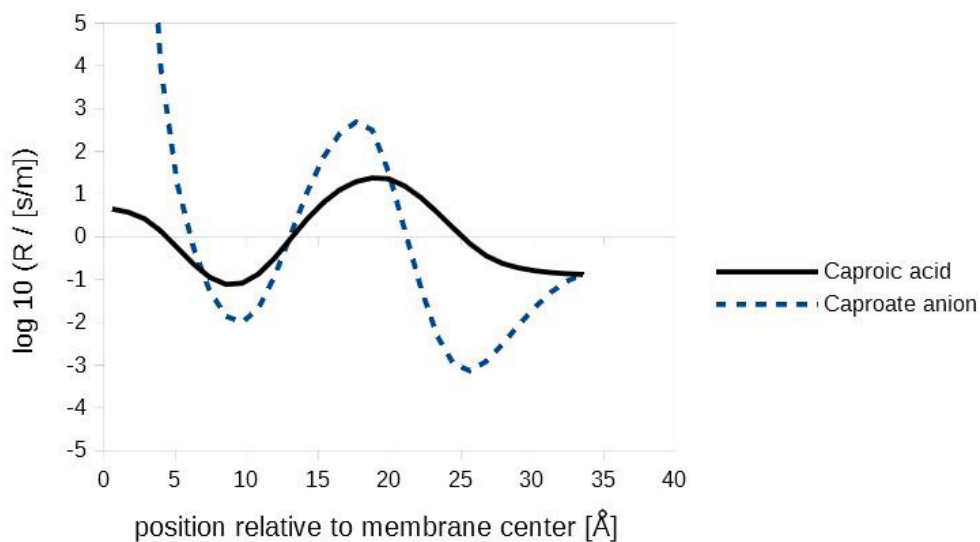


1  
2  
3 **Figure 1.** COSMO<sub>perm</sub> free energy profiles of caproic acid (black line) and the corresponding  
4 caproate anion (blue line): a) free energy profiles in [kJ/mol] units, top; b) resistance profiles in  
5 [s/m] units, bottom. On the left hand side is the central alkyl part of the membrane, on the right  
6 [s/m] units, bottom. On the left hand side is the central alkyl part of the membrane, on the right  
7 hand side the water phase.  
8  
9  
10  
11  
12  
13

14 **Figure 1a.**



35 **Figure 1b.**



1  
2  
3 **Figure 2.** COSMOperm free energy profiles in [kJ/mol] profiles of aspirin, sulfasalazine and  
4 lincomycin (black line, red line and blue line, respectively) with a significant second energy barrier  
5 in the polar head group region, in addition to the membrane interior.  
6  
7  
8  
9

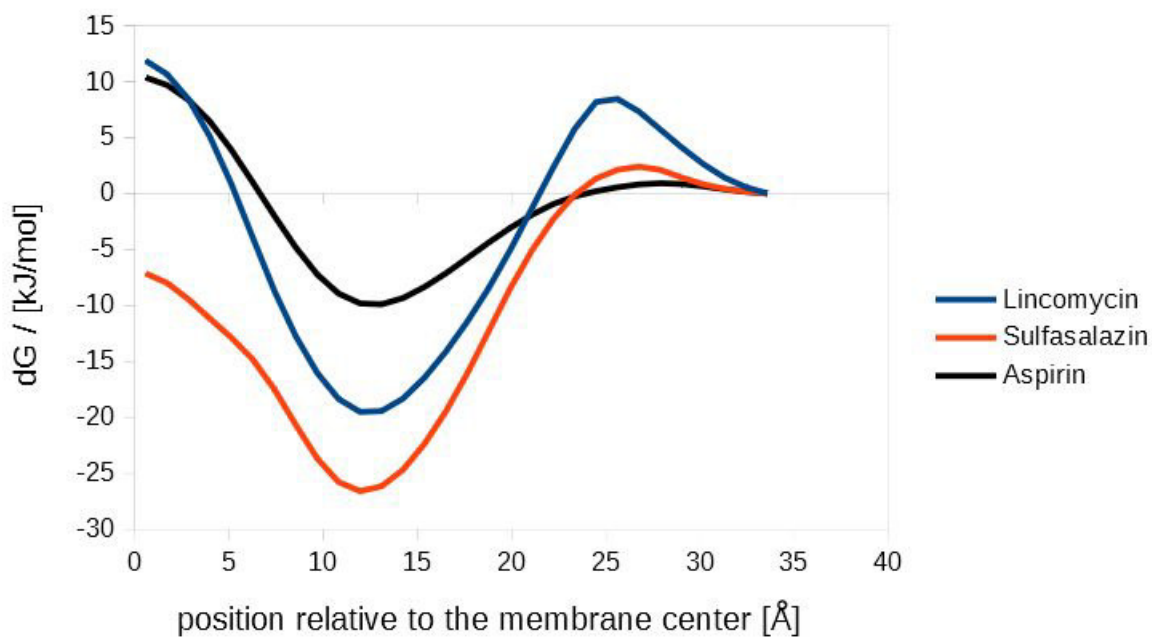


**Figure 3.** Experimental permeabilities and permeabilities predicted by COSMOperm; neutral compounds in black (square), anions in blue (circles).

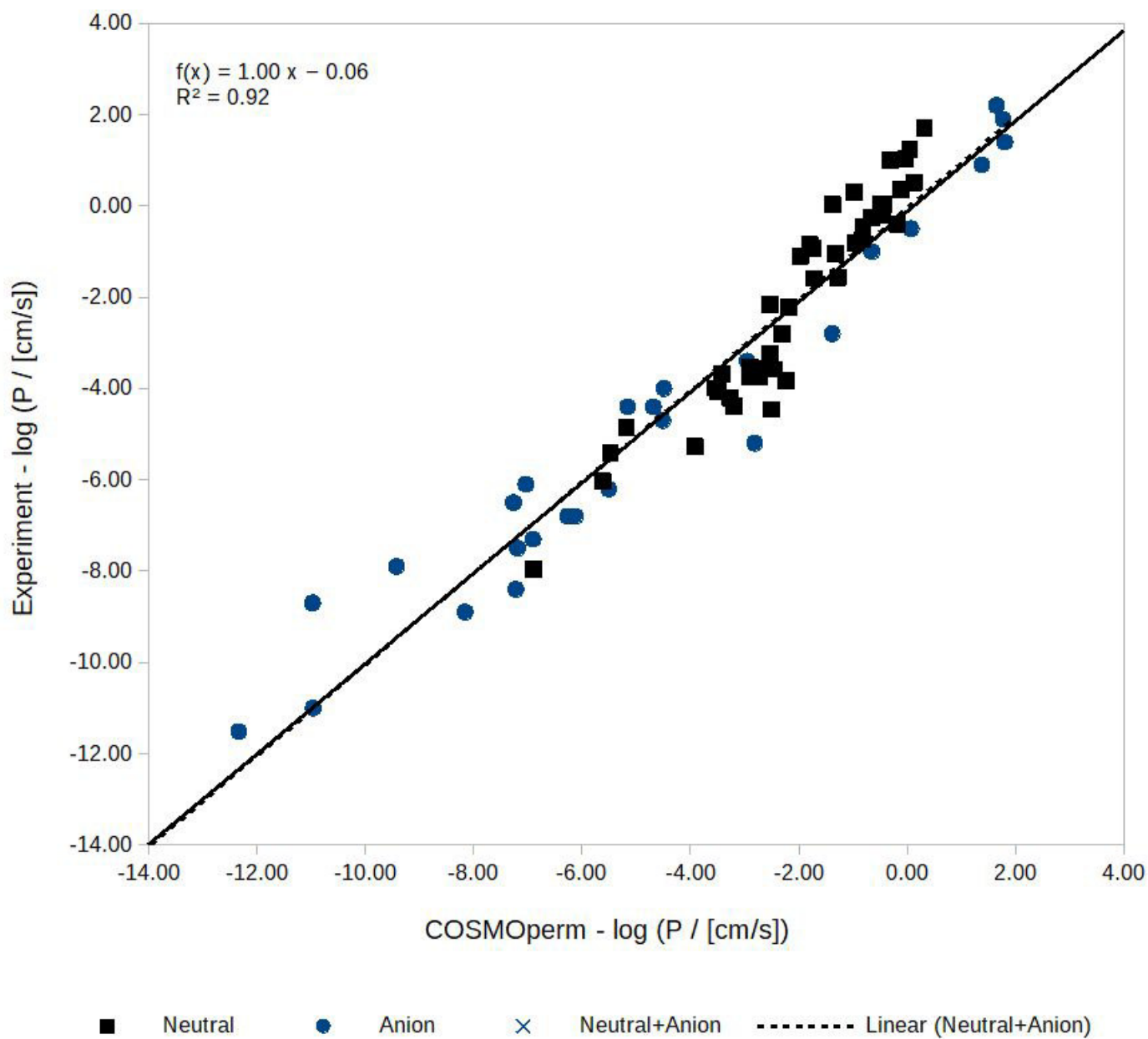


**Figure 4.** Experimental and predicted cation permeabilities for a) all layers (top); or b) for the well-to-well, innermost 24 membrane layers (bottom). The slope of 0.59 was extracted by a global linear fit, and the individual offsets of the depicted correlations correct for the overestimation of membrane permeability depending on the membrane type. Crossed symbols were not considered in the fit (see text).

**Figure 4a.**

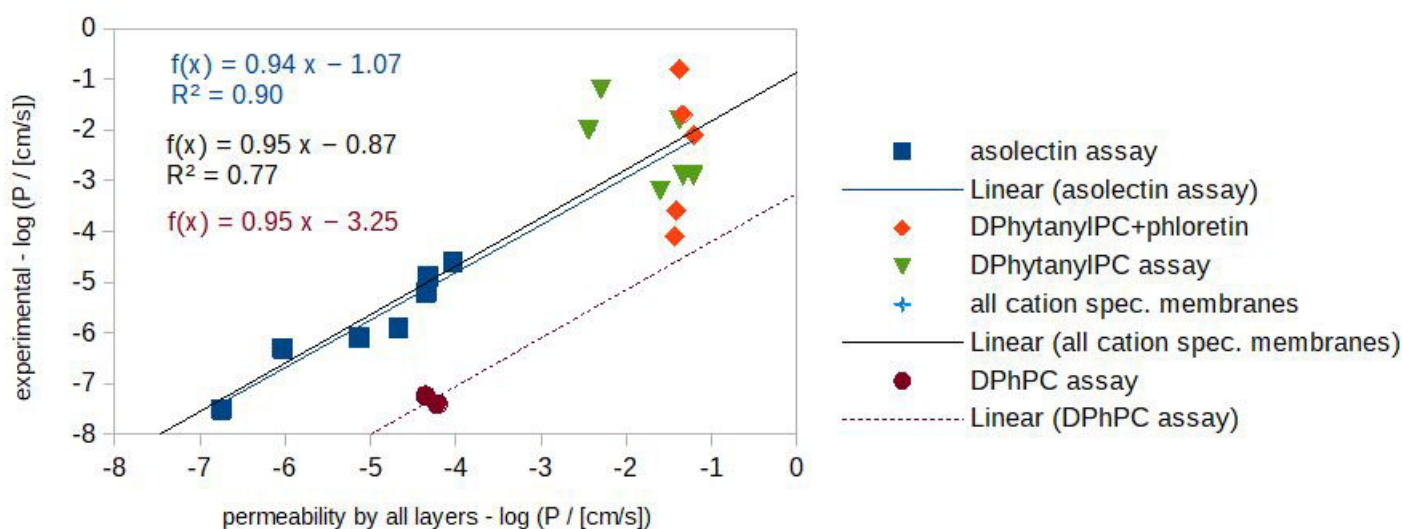
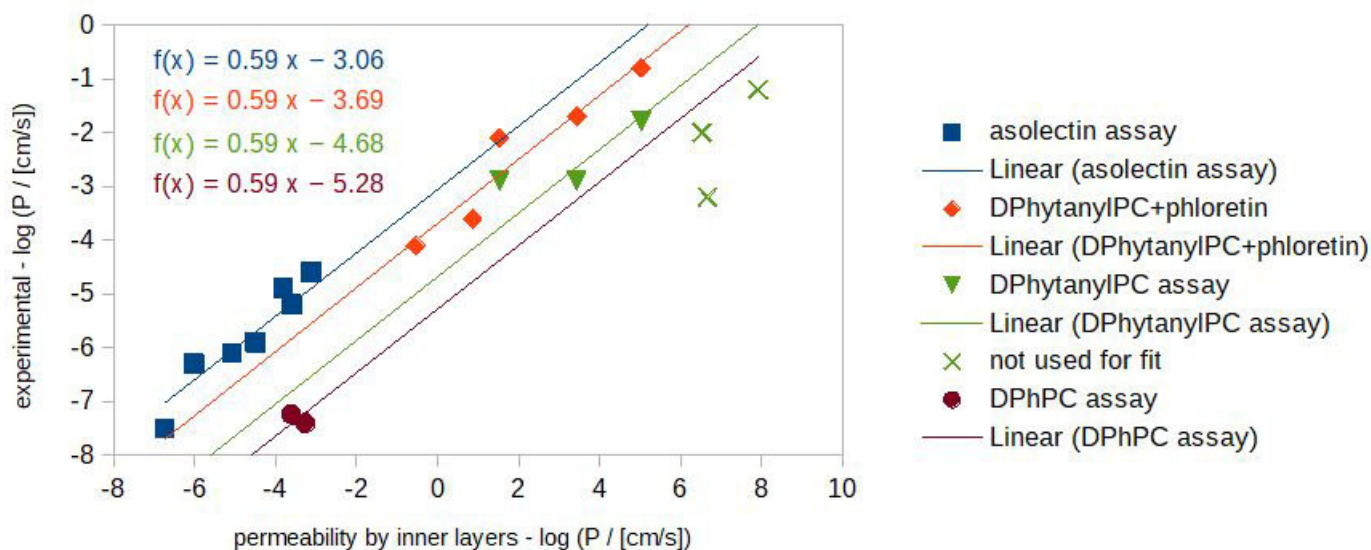


**Figure 4b.**



1  
2  
3 **Figure 5.** pH dependence of experimental effective permeabilities for salicylic acid,<sup>27</sup> and  
4 corresponding permeabilities predicted by COSMOperm. The dotted line shows the experimental  
5 pH dependence derived by the ion flux, which is not corrected for effects introduced by the  
6 unstirred water layer (UWL). The COSMO surfaces are shown for the neutral (left) and  
7 deprotonated state (right), keeping in mind that the permeability value is dominated by the neutral  
8 state at all pH values.  
9  
10  
11  
12  
13  
14  
15  
16  
17  
18  
19

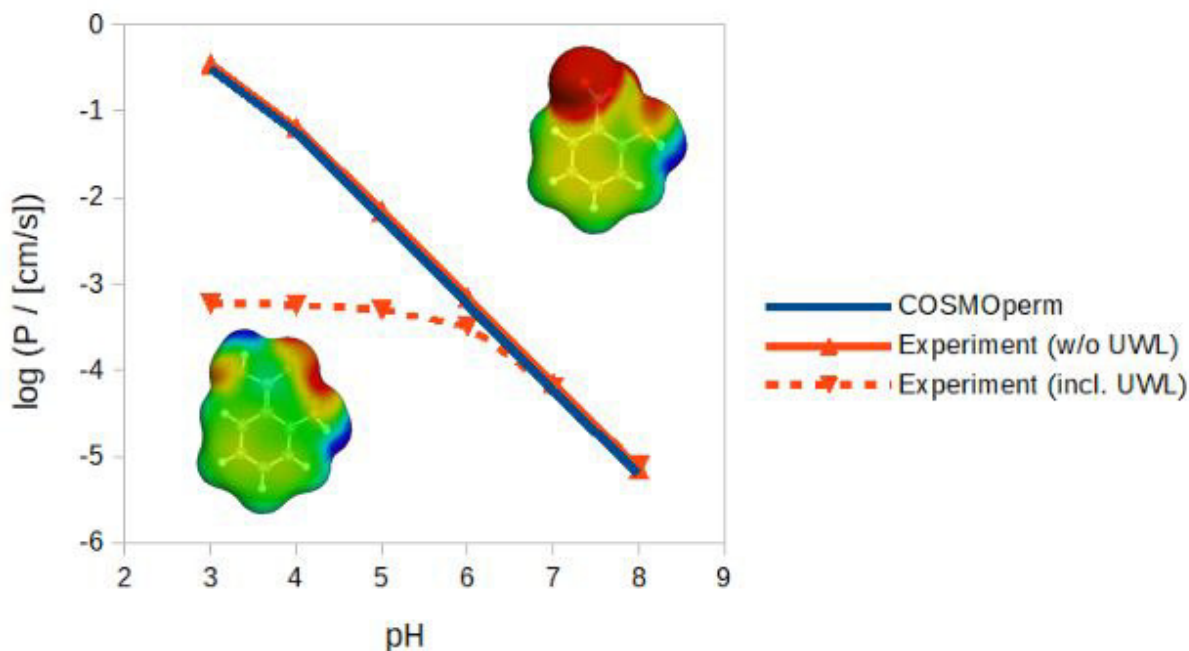


**Table 1.** Set of Experimental (“Exp.”) and Predicted (“Pred.”) Phospholipid Bilayer Membrane Permeabilities for Neutral Compounds and Ions in  $\log_{10}([\text{cm/s}])$  units.

Name	Neutral log (P / [cm/s])			Ion log (P / [cm/s])					
	Exp. <sup>a</sup>	TZVPD -FINE	TZVP	Exp. Anion <sup>b</sup>	Exp. Cation <sup>c</sup>	Pred. <sup>d</sup>	TZVPD -FINE	TZVP	Push- Pull
1,2-ethanediol	-4.1	-3.5	-3.2						
1,2-propanediol	-3.6	-2.7	-2.3						
1,4-butanediol	-3.6	-2.4	-2.4						
2-(2-methyl-2-propanyl)-4,6-dinitrophenol ( <i>dino2terb</i> )		-0.3	0.4	-4.0		-4.5	-2.0	-4.0	yes
2-butan-2-yl-4,6-dinitrophenol ( <i>dinoseb</i> )		-0.3	0.5	-4.4		-5.2	-2.7	-4.6	yes
2,4-dinitrophenol		-0.6	-0.1	-6.5		-7.3	-4.8	-6.8	yes
2,4,6-tribromophenol		-0.1	0.4	-7.3		-6.9	-6.9	-6.4	no
2,4,6-trinitrophenol	-0.4 <sup>q</sup>	-0.2	0.4	-4.1		-6.1	-3.6	-3.6	yes
2,4,6-trinitro-N-(2,4,6-trinitrophenyl)aniline ( <i>DPA</i> )		0.1 <sup>r</sup>	1.6	0.9		1.4	1.4	-3.3	no
2'-deoxyadenosine	-6.0	-5.6	-4.8				-17.8	-12.6	no
2',3'-dideoxyadenosine	-4.2	-3.3	-3.0				-11.8	-9.9	no
3,4-dinitrophenol		-1.4	-0.2	-7.5		-7.2	-4.7	-6.3	yes
3,5-dibromo-2-(2,4-dibromophenoxy)phenol		0.6	1.5	-5.2		-2.8	-2.8	-3.5	no
3,5-dichlorophenol		0.1	0.4	-7.9		-9.4	-9.4	-9.0	no
4-nitro-2-(trifluoromethyl)-benzimidazol		-1.3	-0.8	-6.1		-7.0	-4.6	-5.9	yes
4-nitrophenol		-1.2	-0.6	-8.9		-8.2	-5.7	-9.5	yes
5,6-dichloro-2-(trifluoromethyl)-1H-benzimidazole ( <i>DTFB</i> )	0.3 <sup>m</sup>	-1.0	-0.4				-8.1	-9.1	no
9-anthracenecarboxylic acid	0.5	0.1	0.4				-12.8	-15.0	no
acetamide	-3.7	-3.4	-4.0						
acetic acid	-2.2	-2.2	-2.0				-19.8	-21.8	no
adenine	-4.9	-5.2	-4.7				-14.2	-12.7	no
alpha-carbamoyl- <i>p</i> -toluic acid	-4.4	-3.2	-3.7				-9.7	-17.0	no
alpha-carboxy- <i>p</i> -toluic acid	-3.7	-2.9	-2.2				-11.1	-16.1	no
alpha-chloro- <i>p</i> -toluic acid	-0.2	-0.5	-0.2				-14.1	-15.5	no
alpha-cyano- <i>p</i> -toluic acid	-1.6	-1.3	-1.5				-12.1	-16.2	no
alpha-hydroxy- <i>p</i> -toluic acid	-2.8	-2.3	-1.9				-14.9	-17.4	no
alpha-methoxy- <i>p</i> -toluic acid	-0.5	-0.8	-0.5				-14.8	-16.3	no
alpha-naphthoic acid	0.4	-0.1	0.0				-14.4	-16.4	no
ascorbic acid	-8.0 <sup>e</sup>	-6.9	-5.2	$\leq -11.5^e$		-12.3	-12.3	-14.7	no
aspirin	-0.8 <sup>f</sup>	-1.0	-0.6				-15.0	-16.5	no
benzoic acid	-0.3	-0.7	-0.5				-16.7	-17.8	no

1										
2										
3	beta-naphthoic acid	1.2	0.0	0.1			-14.7	-16.1	no	
4	bis(fluorosulfonyl)amide		0.0	0.5	-4.7		-4.5	-4.5	-2.4	no
5	bromoxynil		-0.6	-0.3	-6.2		-5.5	-3.0	-6.1	yes
6	butyltriphenylphosphonium					-5.9	-5.8	-4.7		no
7	butyric acid	-1.1	-1.3	-1.0				-18.5	-20.2	no
8	carbonyl cyanide <i>p</i> -	1.7 <sup>j</sup>	0.3	0.0				-1.8	-2.7	no
9	trifluoromethoxyphenylhydrazone ( <i>FCCP</i> )									
10	carbonylcyanide <i>m</i> -chlorophenylhydrazone	1.0 <sup>l</sup>	0.0	-0.3	-3.4		-3.0	-3.0	-3.4	no
11	( <i>CCCP</i> )									
12	codeine	-0.9	-1.8	-1.2				-14.8	-7.9	no
13	coumachlor		-1.1	-0.2	-6.8		-6.1	-3.6	-7.1	yes
14	cyano(triphenyl)boranuide			-2.2	-2.8		-1.4	-1.4	-3.2	no
15	ethylamine	-0.9 <sup>g</sup>	-1.7	-2.1				-16.7	-12.9	no
16	ethyltriphenylphosphonium					-6.3	-6.7	-6.0		no
17	flufenamic acid		0.4	0.9	-6.8		-6.3	-6.3	-9.4	no
18	formamide	-4.0 <sup>h</sup>	-3.5	-4.4						
19	formic acid	-2.2 <sup>i</sup>	-2.5	-2.7				-18.5	-20.9	no
20	glycerol	-5.3	-3.9	-3.3						
21	hexanoic acid	0.0	-0.5	-0.3				-17.1	-19.0	no
22	hexyl(triphenyl)phosphonium					-4.6	-4.9	-4.0		no
23	histamine	-4.5	-2.5	-2.9				-13.8	-6.7	no
24	hydrocortisone	-3.3	-2.5	-1.5						
25	hydrocortisone-21-pimelamide	-3.7	-2.7	-2.9					-10.9	no
26	methylamine	-1.1 <sup>g</sup>	-2.0	-2.4				-17.3	-14.4	no
27	methyltriphenylphosphonium					-7.5	-7.1	-6.7		no
28	<i>n</i> -dodecyl trinaphthyl phosphonium					-3.2 <sup>p</sup>	-0.7	-1.6		no
29	<i>n</i> -dodecyl tri(3,5-dimethylphenyl)					-1.2 <sup>p</sup>	0.1	-2.3		no
30	phosphonium									
31	<i>n</i> -dodecyl tri( <i>p</i> -chloro-phenyl)					[-3.6] <sup>p</sup>	[-3.2]	-1.4		no
32	phosphonium									
33	<i>n</i> -dodecyl tri( <i>p</i> -fluorophenyl) phosphonium					[-4.1] <sup>p</sup>	[-4.0]	-1.4		no
34	<i>n</i> -dodecyl tri( <i>p</i> -methoxyphenyl)					-2.9 <sup>p</sup>	-2.6	-1.3		no
35	phosphonium					[-1.7]	[-1.6]			
36	<i>n</i> -dodecyl tri( <i>p</i> -tolyl) phosphonium					-1.8 <sup>p</sup>	-1.7	-1.4		no
37						[-0.8]	[-0.7]			
38	<i>n</i> -dodecyl triphenyl phosphonium					-2.9 <sup>p</sup>	-3.8	-1.2		no
39						[-2.1]	[-2.8]			
40	<i>n</i> -dodecyl tri(2,4,6-trimethylphenyl)					-2.0 <sup>p</sup>	-0.8	-2.4		no
41	phosphonium									
42	<i>p</i> -toluic acid	0.0	-0.4	-0.2				-16.8	-17.6	no
43	pentachlorophenol		0.0	0.5	-4.4		-4.7	-4.7	-4.6	no
44	perchloric acid		-1.0	-0.5	-8.7		-11.0	-11.0	-8.1	no
45	phloretin	-3.6	-2.8	-1.4				-8.2	-9.7	no
46	prednisolone	-3.8	-2.2	-1.8						
47										
48										
49										
50										
51										
52										
53										
54										
55										
56										
57										
58										
59										
60										

1										
2										
3	propionic acid	-1.6	-1.7	-1.4			-19.0	-20.8	no	
4	salicylic acid	-0.1	-0.5	0.0	-11.0		-11.0	-11.0	-12.5	no
5	tetrachlorotrifluoromethylbenzimidazole	1.0 <sup>k</sup>	-0.3	0.2						
6	( <i>TTFB</i> )									
7	tetraethylboranuide				-1.0		-0.7	-0.7	-0.3	no
8	tetrakis(3-trifluoromethylphenyl)boranuide				2.2		1.6	1.6	1.8	no
9	tetrakis(4-chlorophenyl)boranuide				1.9		1.8	1.8	1.8	no
10	tetrakis(4-fluorophenyl)boranuide				1.4		1.8	1.8	1.8	no
11	tetraphenylarsonium					-7.2 <sup>n</sup>	-7.2	-4.2		no
12	tetraphenylborate				-0.5		0.1	0.1	0.8	no
13	tetraphenylphosphonium					-5.2 <sup>o</sup>	-5.2	-4.0	-2.6	no
14	theophylline	-3.5	-2.9	-3.3				-8.8	-13.5	no
15	triethylamine	0.0	-1.4	-0.8				-14.5	-4.8	no
16	triphenylamylphosphonium					-4.9	-5.4	-4.3		no
17	triphenylpropylphosphonium					-6.1	-6.1	-5.1		no
18	tryptamine	-0.7	-0.8	-1.1				-14.4	-11.0	no
19	Urea	-5.4	-5.5	-6.4						
20	warfarin		-1.1	-0.4	-8.4		-7.2	-4.7	-8.3	yes

<sup>a</sup> Ref. (3), if not indicated otherwise; experiments: phosphocholin membranes. <sup>b</sup> Ref. (31), if not indicated otherwise; experiments: phosphocholin membranes. <sup>c</sup> Ref. (53) asolectin membrane, if not indicated otherwise. <sup>d</sup> Predictions at TZVPD-FINE level: including push-pull effect constant (-2.5), if applicable, as indicated by last column. Cation predictions are corrected for slopes and intercepts, as indicated by **Figure 4b**. <sup>e</sup> Ref. (20). <sup>f</sup> Ref. (58). <sup>g</sup> Ref. (5). <sup>h</sup> Ref. (59). <sup>i</sup> Ref. (60). <sup>j</sup> Ref. (36). <sup>k</sup> Ref. (61). <sup>l</sup> Ref. (62). <sup>m</sup> Ref. (63). <sup>n</sup> Ref. (64) DOPC membrane in hexadecane. <sup>o</sup> Ref. (53), and new measured value: -7.2 DPhPC membrane (pred.: -7.5). <sup>p</sup> Ref. (51) DPhytanylPC membrane, values in [brackets]: DPhytanylPC including phloretin. <sup>q</sup> Ref. (65). <sup>r</sup> Neutral state limited by the polar headgroups at TZVPD-FINE level, for this reason the permeability value of the ion without polar headgroup limitation is predicted to be higher, even though the free energy of the latter is still higher in the – here not rate-limiting – alkyl part (see Figure S4.5 in the supporting information).

**Table 2.** COSMO<sub>perm</sub> Statistics for Different Datasets.

Dataset	Model Membrane	TZVPD-FINE					TZVP					
		<i>N</i>	<i>r</i> <sup>2</sup>	<i>rmsd</i>	<i>slope</i>	<i>intercept</i>	<i>rmsd</i> <sup>a</sup>	<i>r</i> <sup>2</sup>	<i>slope</i>	<i>intercept</i>	<i>rmsd</i>	<i>rmsd</i> <sup>a</sup>
Neutral	DMPC	45	0.91	0.84	1.29	+0.56	0.69	0.81	1.21	+0.17	1.06	0.98
Anions <sup>b</sup>	DMPC	27	0.94	1.00	0.90	-0.47	0.93	0.89	0.83	-0.81	1.40	1.26
								[0.93]			[1.17]	[0.93]
Neutral + Anions <sup>b</sup>	DMPC	72	0.92	0.90	0.99	-0.06	0.90	0.87	0.92	-0.39	1.20	1.17
								[0.90]			[1.10]	[1.06]
Cations <sup>c</sup>	DMPC	16	0.81	NA	0.95	-0.87	0.93					
Cations <sup>d</sup>	DMPC (inner layers)	16	0.90	NA	0.59	assay dependent	0.82					
Selected anions	DMPC+ chlorodecane	6	0.96	1.57	0.81	+0.69	0.52	0.92	1.07	+0.09	0.88	0.88

<sup>a</sup> Corrected for slope and intercept; <sup>b</sup> Values in brackets without DPA, the largest outlier at TZVP level; <sup>d</sup> Cation data measured by a set of assays. The *r*<sup>2</sup> and *rmsd* values shown use a slope of 0.95 and an intercept of -0.87 for all membranes adapted to cations and -3.25 for DPhPC/DOPC membranes (see **Figure 4a**) <sup>d</sup> Cation data measured by a set of assays. The *r*<sup>2</sup> and *rmsd* values shown use a slope of 0.59 and assay dependent intercepts (see **Figure 4b**).

**Table 3.** Set of Experimental Ions Permeabilities in  $\log_{10}(\text{cm/s})$  units in a Chlorodecane/DMPC System, Predicted Permeabilities in a Chlorodecane/DMPC Model System (TZVP) and Differences to the DMPC Model System (TZVP).

Compound <sup>a</sup>	Permeability in $\log_{10}(\text{cm/s})$			
	Experiment <sup>b</sup>	DMPC+ Chlorodecane	DMPC (pure)	Difference
CCCP anion	-0.50	-1.05	-3.39	-2.34
DTFB anion	-1.50	-1.16	-3.89	-2.73
FCCP anion	0.30	-0.42	-2.70	-2.28
perchlorate anion	-5.80	-3.95	-8.12	-4.17
S-13 anion	0.80	0.79	-2.56	-3.35
thiocyanate anion	-5.80	-6.36	-11.49	-5.13

<sup>a</sup> Abbreviations are listed in **Table 1**; S-13: 3-tert-butyl-5-chloro-N-(2-chloro-4-nitrophenyl)-2-hydroxybenzamide. <sup>b</sup> Ref. (31), table S7, additional data listed in the supporting information.